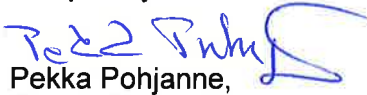


Basic approaches and goals for crevice corrosion modelling

Authors: Maija Raunio

Confidentiality: Public

Report's title	
Basic approaches and goals for crevice corrosion modelling	
Project name	Project number/Short name
FIMECC/BSA/P1SP1GPRO	86433
Author(s)	Pages
Maija Raunio	49/0
Keywords	Report identification code
Crevice corrosion, corrosion modelling	VTT-R-02078-15
Summary	
<p>In this literature review Basic approaches and goals for crevice corrosion modelling, crevice corrosion in general and factors affecting it are described. The main focus is on approaching the modelling perspective of crevice corrosion, and studying the existing methods and models (empirical, statistical, and mechanistic) used for this kind of modelling. The idea is trying to distinguish the most representative and realistic crevice corrosion models on the field.</p> <p>All of the existing models use simplifications and assumptions to be able to describe the general phenomenon. The coupled environment theory, which takes into account the interaction between the crevice and the external surfaces, has model potential for predicting the crevice corrosion system. Modelling tools (FEM, COMSOL and other developed platforms) are being utilized to minimize the work load needed in developing the models. The flexibility and functionality of these platforms needs to be up-to-dated. Statistical perspective in crevice corrosion modelling is needed to get more reliable results. The modelling and understanding of crevice corrosion has challenges yet, since the processes taking part in crevice corrosion are very dynamic and complex.</p>	
Confidentiality	Public
Espoo, 11.5.2015	
Written by	Reviewed by
 Maija Raunio, Research scientist	 Leena Carpen, Principal scientist
	Accepted by
	 Pekka Pohjanne, Deputy Head of Research Area
VTT's contact address	
VTT Technical Research Centre of Finland, P. O. Box 1000, FI-02044 VTT, Finland	
Distribution (customer and VTT)	
1 piece: FIMECC Portal	
1 piece: VTT Oy	
<p><i>The use of the name of VTT Technical Research Centre of Finland Ltd in advertising or publication in part of this report is only permissible with written authorisation from VTT Technical Research Centre of Finland Ltd.</i></p>	

Preface

This literature review was performed during the summer and autumn of 2014 as a part of TEKES jointly-funded project “Finnish Metals and Engineering Competence Cluster - Breakthrough steels and applications”. A description has been given of the most common factors affecting crevice corrosion modelling, and the challenges involved. The idea was to discover the existing approaches and methods for crevice corrosion modelling, and distinguish the most potential models describing variety of metal-environment combinations.

Espoo 11.5.2015

Author

Contents

Preface.....	2
Contents.....	3
1 Introduction.....	5
2 Mechanisms of crevice corrosion.....	5
2.1 Passivity.....	5
2.2 Pitting corrosion.....	9
2.3 Crevice corrosion.....	11
2.4 Factors affecting crevice corrosion.....	12
2.4.1 Oxide films.....	12
2.4.2 Alloying elements in metals.....	12
2.4.3 Repassivation.....	12
2.4.4 Geometry.....	13
2.4.5 Temperature, pH and chemical environment.....	13
2.5 Theories of crevice corrosion.....	14
2.5.1 Critical IR Drop theory (IRDT).....	14
2.5.2 Critical crevice solution (CCS) theory.....	16
2.5.3 Coupled environment theory.....	17
2.5.4 Repassivation potential approach.....	18
2.5.5 Metastable pitting theory.....	19
3 Crevice corrosion modelling.....	19
3.1 Structure and challenges of crevice corrosion modelling.....	20
3.2 Relevant electrochemical reactions and equations in crevice corrosion modelling.....	22
3.2.1 Electrochemical reactions.....	22
3.2.2 Equations.....	25
3.3 Experimental work on crevice corrosion.....	27
3.3.1 Alavi and Cottis experiment.....	27
3.3.2 Valdes-Mouldon experiment.....	28
3.3.3 Thiosulphate entrapment experiment.....	29
3.3.4 Pitting as a precursor of crevice corrosion.....	29
3.3.5 Passive dissolution experiment.....	30
3.3.6 Calculating coupling current.....	31
3.4 Empirical crevice corrosion models.....	31
3.4.1 Empirical model for localized corrosion.....	31
3.5 Statistical crevice corrosion models.....	31
3.6 Mechanistic crevice corrosion models.....	32
3.6.1 Point defect model (PDM).....	32
3.6.2 Coupled environment models.....	33
3.6.3 Critical crevice depth method.....	34
3.6.4 Combined IR drop theory and CCS model.....	35
3.6.5 Computational model for incubation of crevice corrosion.....	36
3.6.6 FEM model of the propagation of crevice corrosion and pits.....	37
3.6.7 ALE (arbitrary Lagrangian–Eulerian) model.....	40
3.6.8 Cathodic focusing (CF) model.....	42

3.6.9 Repassivation potential model	42
4 Discussion and conclusions	43
5 Summary	46
References.....	47

1 Introduction

The difference between uniform and localized corrosion can be seen clearly when the corrosion rates of corroding metals are compared. Uniform corrosion proceeds about the same rate over the whole surface of the metal exposed to the corrosive environment, but localized corrosion proceeds at higher rates at different areas of the metal surface due to heterogeneities in the metal, the environment or in the geometry of the structure. Therefore localized corrosion results in worse damage than uniform corrosion because it can lead to perforation in a shorter period of time. Localized corrosion covers such phenomena as pitting corrosion, crevice corrosion, intergranular corrosion, stress corrosion cracking and corrosion fatigue. From these types especially pitting and crevice corrosion are dangerous, since it has been observed that other forms of localized corrosion, like stress corrosion cracking and corrosion fatigue, often initiate from pits and crevices. Prevention of localized corrosion is of great interest among corrosion scientists and engineers due to massive technical and economic harm that a corrosion induced failure can cause. [1-3]

When prevention of localized corrosion is desired, modelling has a vital role. Nowadays more and more modelling is needed to prevent the possibility of catastrophic failures in industry, and the required level of modelling is expected to be comprehensive, extending from atomistic to continuum scale including all the processes of interest. A predictive tool to link the material and environmental properties with the final component performance would provide an attractive assistance for design. In practise such model could determine when localized corrosion is likely to occur, maximum crevice or pit penetration depths theoretically possible under specific conditions, and the relationship between electrolyte composition and propagation of crevice corrosion. [4-9]

Developing of a modelling tool naturally requires deep understanding on localized corrosion and the associated processes on different scales and on the behaviour of the overall system. Despite the investigations that have been made, the prediction of localized corrosion is still a challenging task. Reasons for the difficulty are the small dimensions of events, high reaction rates, and heterogeneous surfaces, which make the system highly dynamic with rapidly moving boundaries and rapidly changing chemistries and potentials. It is not possible to predict exactly when and where the passive film breakdown will occur, hence the high-resolution observation of initiation events is extremely difficult. [5,7]

In this review crevice corrosion and its prediction via modelling is of interest. The study goes first through crevice corrosion and its features in general, and theories describing the mechanisms of crevice corrosion. In the modelling part the performed experiments, developed empirical, statistical and mechanistic models are described. The idea is trying to distinguish the most representative and realistic crevice corrosion models existing in the field.

2 Mechanisms of crevice corrosion

Understanding of crevice corrosion starts by investigating the reasons for crevice corrosion. Passivity and pitting are closely linked to the crevice corrosion phenomena, and they explain what needs to be taken into account when considering crevice corrosion and its modelling. In the next chapters passivity, pitting and crevice corrosion in general are reviewed. Also the factors affecting crevice corrosion and few existing theories explaining crevice corrosion mechanism are shortly described.

2.1 Passivity

Passivity is a state of low corrosion rate under a high anodic driving force, or potential, by the presence of an interfacial solid film, usually an oxide. The oxide film itself is formed

anodically through a mechanism very similar to the corrosion process, and decreases the rate of further oxidation (corrosion and further passivation) by forming a barrier between the metal surface and its environment. Even an extremely thin film is enough to procure passivity of metals. The passive state is illustrated by a classical polarization curve prepared potentiostatically or potentiodynamically (Fig. 1). As the potential is raised (in anodic or positive sense) above the equilibrium potential between the metal and its dissolved ions, the driving force towards oxidation increases and the rate of dissolution increases, creating an exponential rise of current with potential according to the Tafel equation (Chapter 3.2.2.1, equation 2). When the potential is high enough, a dramatic reduction in the dissolution rate occurs, and the rate of dissolution remains low with further increase in potential. This latter state is the passivity state (Fig. 1, range CD) and the minimum potential at which the low oxidation rate exists is the passivation potential. At the passive state the oxidation rate is nearly independent of potential. However some surface films, while displaying all the qualitative properties of passivity with respect to the polarization curve, allow a high corrosion current to pass, and cannot therefore be regarded as passive films. In the absence of an applied potential, the electrons generated by the anodic oxidation of the metal will be used by a cathodic reaction which occurs on the passive metal surface itself. In aqueous systems the cathodic reaction is generally the reduction of dissolved oxygen or the reduction of water to hydrogen (or both simultaneously, depending upon the potential involved) occurring on the passive oxide surface. [2]

The state of passivity is never perfect, and a passive metal always corrodes at a specific rate, though this rate may be very low (depends on application). It is generally important to know the passive corrosion rate, which is determined as the passive current density, i_{pass} , through polarization experiments. One should keep in mind that passive metals are thermodynamically unstable: they possess a kinetic stability created by the solid interfacial film, and without which corrosion would occur. Passivity normally exists within a defined potential range, below which the metal may activate and corrode, and above which it may trans-passivate and corrode. The potential range is characteristic of the metal/environment system, and of the available cathodic reaction. Because all anodic processes occurring through the passivating film, including film growth itself, are controlled by the ionic movement inside the film, a low ionic conductivity to metal cations as well as oxide ions is beneficial to passivity. Oxides of high ionic conductivity would grow to be thick, and thick oxide films are more likely to be mechanically unstable, because they are more crystalline and defective. The passivating film thickness is also controlled by the rate of dissolution of the oxide into the electrolyte. The Pourbaix diagrams (e.g. the equilibrium potential - pH equilibrium diagrams) constructed from thermodynamic data, show how a metal in a natural environment (e.g. iron in water of given chloride ion concentration) may give rise to general corrosion, pitting, passivity or immunity depending on the pH and potential. [2]

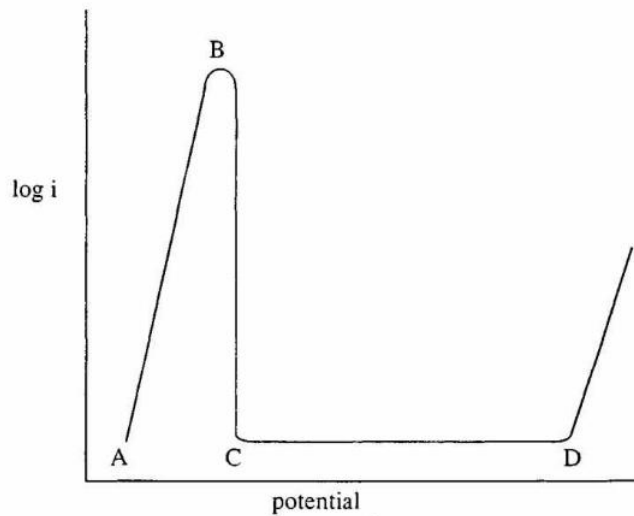


Figure 1. Schematic anodic polarization curve for a metal. Region AB describes active dissolution of the metal. BC is the active/passive transition, with passivation starting at B. Passivation is complete only at potentials higher than C. The metal is passive over the range CD. [2]

From anodic polarization curves two characteristics can be established: the pitting potential E_p or E_{pit} and the repassivation potential E_{rp} (Fig. 2). Also the corrosion potential E_{corr} (the potential between electrode and a reference electrode in a corrosive environment) is defined in Fig. 2. E_p is represented by a sudden increase of the current, and E_{rp} is associated with a drop in current due to pit repassivation. There are several definitions for E_p : the potential above which stable pits propagate or a necessary potential to maintain a salt film inside a pit, a potential at which pit solution composition is aggressive enough to keep the passive film locally unstable and thus prevent repassivation, or a minimum potential for metastable pits to become stable. E_{rp} is defined as the potential, below which no metastable and stable pitting occurs, and above which metastable pits can form and already existing pits can propagate. It was also suggested that E_{rp} is the minimum required potential to maintain the critical environment inside a propagating pit. Both E_{pit} and E_{rp} were found to be dependent on the method of their determination. [10]

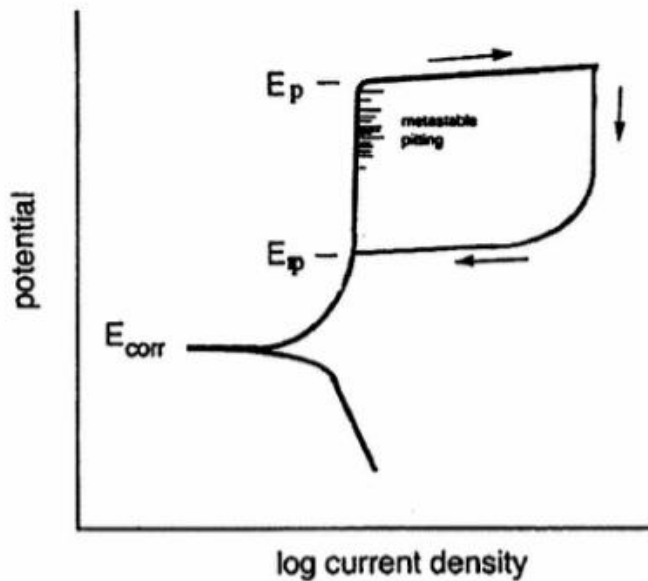


Figure 2. Schematic representation of anodic polarization curves for a metal immersed in a solution containing aggressive ions. Potentiostatic measurements conducted (a) upward, (b) backward. E_p , E_{corr} and E_{rp} are defined in the curve. [1]

It has been proposed that passivity loss leading to localized corrosion or pitting in passive metals results from a variety of different mechanisms. Three main mechanisms are: 1) the penetration mechanism (Fig. 3), 2) the film breaking mechanism (Fig. 4), and 3) the adsorption mechanism (Fig. 5). In penetration mechanism different aggressive ions are found to penetrate the passive film more readily than others. The incorporation of ions contaminates the film and leads to higher ionic conductivities along the penetration paths, which then eventually results in pitting. Film breakdown mechanism requires breaks (e.g. blistering, accumulation of vacancies, micro-capillary formation and the crack-heal mechanism) within the film to give direct access of anions to the unprotected metal surface. The adsorption mechanism starts with adsorption of aggressive anions at the oxide surface, which catalytically enhances the transfer of metal cations from the oxide to the electrolyte. This effect leads to thinning of the passive layer with possible final total removal and the start of intense localized dissolution. The theory assumes that the passive film is a layer of adsorbed oxygen and that pits initiate at sites where Cl^- ions displace the oxygen. [10]

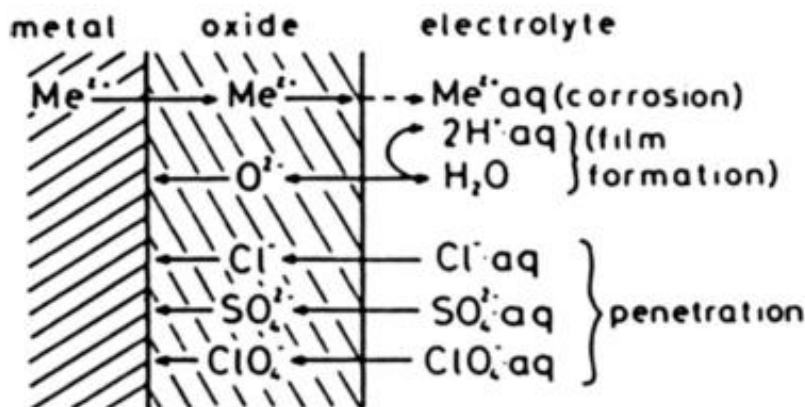


Figure 3. Penetration mechanism and phase diagram of a passive film with related processes of ion and electron transfer within the film and at its phase boundaries. [10]

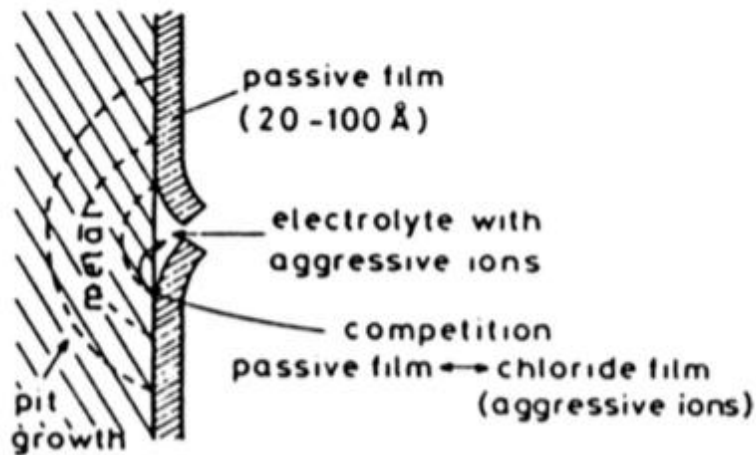


Figure 4. Mechanical film breakdown mechanism and related competing processes. [10]

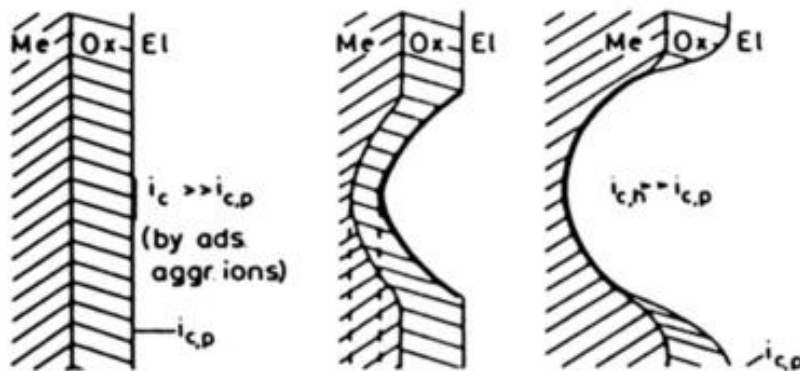


Figure 5. Adsorption mechanism with increased local transfer of metal ions and related corrosion current density, i_c , caused by complexing aggressive anions leading to thinning of the passive layer and increases in field strength and final free corrosion current density $i_{c,h}$ within the pit. [10]

2.2 Pitting corrosion

Pitting corrosion is caused by local dissolution leading to the formation of cavities in passivated metals exposed to an aqueous, nearly neutral solution containing an aggressive anion, usually Cl^- . The anode of the corrosion reaction is situated in the pit and the cathode usually on the surrounding surface. The characteristic feature of this type of localized corrosion is a sudden breakdown of the passive film at the pitting potential E_p , above which pits are growing, but below which only nucleated pits can develop (Chapter 2.1). Intensive studies of metastable pits, formed in the region of potentials below E_p and above E_{rp} , have increased knowledge on the initiation step of pit growth. The measurements of these two characteristic potentials and metastable pits in a function of different external (environmental composition, temperature) and internal factors (alloy and passive film composition, etc.) reveal the influence of separate factors on the susceptibility of metals to pitting and crevice corrosion. It is assumed that the metastable pits cannot grow until E_p is reached. This indicates that film breakdown is a necessary but not sufficient condition for pit growth to occur. It is also assumed that there are two distinct processes before stable pit formation occurs: pit nucleation and growth of the metastable pit. Impurities in the substrate and repassivation process in chloride solutions have a substantial influence for breakdown of the film. A general opinion is that in the pit nucleus the salt film already exists. It is not known why the transition from metastable to stable pits occurs mainly with the formation of crystallographic pits. Either the pit solution within the metastable pit create conditions for an

active dissolution of metal, or the concentrated pit solution (or salt film) already exists, and dilution of the pit occurs during the failure of the pit cover resulting in an active dissolution of the metal. It seems that the second event is more likely, because rather hemispherical metastable pits are observed. [1-3]

When the pit's content is analysed, very concentrated chlorides of dissolved metal cations and very low pH is found. Also a salt film is found at the bottom of the pits, and the pits are usually covered by remnant of passive film together with some metal and corrosion products. All these factors influence the pit development as well as the alloy composition, the concentration of aggressive and nonaggressive substances in the bulk solution outside the pit, and temperature. It has been suggested by Hisamatsu [11] that a critical concentration of ions in the pit electrolyte exists, above which the pit can grow, and below which the pit can be repassivated, independent of the repassivation potential and pit radius. For example for stainless steel in sulfuric acid containing Cl^- ions, this value is 1.8 kmol/m^3 . He also claimed that the local concentration is proportional to the product of the pit current density i \times pit radius r . Galvele [12] claimed that the current density times pit radius must be greater than a critical value in order for the pH at the pit surface to be sufficiently low to maintain active condition for pit growth. When a pit develops in a supersaturated pit solution, a salt film can form. Currently, most of the authors claim that a concentration of Cl^- is more important for stabilizing pit growth than pH level. However, it should be noted that the higher the concentration of chloride ions in the solution, the lower the pH. While several researchers argue that a salt film is necessary, others have shown that a critical level of chloride concentration, below the saturation concentration with respect to the metal salt, is sufficient for pit propagation. [1]

To measure the susceptibility of metals and alloys to pitting, the determination of critical pitting temperature (CPT) and critical crevice temperature (CCT) is a commonly used option. Below a certain CPT, steel does not experience pitting when exposed to an oxidized chloride solution such as FeCl_3 or subjected to a constant anodic potential in an aggressive solution. Below CPT, the current density needed to sustain the pit environment is greater than that required for passivation and thus all metastable pits repassivate, hence there is no stable pitting at any potential below CPT for stainless steel. To determine CPT for a chosen system the test temperature is usually increased in $2.5 \text{ }^\circ\text{C}$ steps every 24 h until pitting occurs. [1,10]

Pitting and crevice corrosion have many similarities. Ranking of alloys in order of crevice corrosion resistance is almost the same as of pitting corrosion, hence the effect of alloying elements and mechanism of their action is the same. Both in pits and in crevices the concentration of metals cations, H^+ and Cl^- , is largely enriched relatively to the bulk solution. Critical pitting potential and CPT exist for pitting and crevice corrosion. Some dissimilarity also exists between pitting and crevice corrosion. In contradiction to crevice corrosion, pitting can initiate at different vulnerable points on a metallic surface to which the surrounding corrosive medium has free access. Crevice corrosion, in contrast, focuses its attack on only a portion of a metallic surface to which the access of the environment is limited by geometric reasons system. Crevice corrosion most often occurs in chloride solutions, like pitting, but crevice corrosion may also occur in other corrosive liquids (e.g., in sulfuric acid). Because of immobility of the solution in the crevice, an exchange between its interior and bulk solution is difficult. The critical potential at which crevice corrosion nucleates is therefore less positive than pitting potential, and in most cases, crevice corrosion initiates more rapidly than does pitting. For this reason, the general opinion is that crevice corrosion is more detrimental than pitting in practice. Note that crevice corrosion occurs in several systems in which pitting corrosion does not occur: Ni in H_2SO_4 , iron in acetic acid + sodium acetate and in sulfuric acid. [1]

2.3 Crevice corrosion

Crevice corrosion is a form of localized corrosion that occurs frequently on metals exposed to stagnant solutions within shielded areas such as holes, gaskets, lap joints and crevices under bolts. Usually the narrow openings or gaps between metal-to-metal or nonmetal-to-metal components can generate crevice corrosion. Also precipitates and metal oxides scales can act as a shielded area promoting crevice corrosion. In some cases crevice corrosion can simply be caused by corrosive liquid being held in the crevice, while surrounding surfaces dry out. Crevice corrosion is usually very difficult to detect and predict due to the size and locations of the corroding crevice. Crevice corrosion can occur on the surface of all kinds of metallic alloys, but passive alloys, i.e., materials with high corrosion resistance, are more prone to crevice corrosion than active materials. Examples of susceptible metals are stainless steels, nickel, titanium and aluminium alloys. [13-15]

In the simplest case, crevice corrosion starts when oxygen differential cell is formed. This can occur when oxygen within the crevice electrolyte is consumed, while the outside surface has access to oxygen and becomes cathodic and the crevice area becomes anodic. During the crevice corrosion process, as the crevice mouth narrows gradually, the mass transfer between crevice solution and bulk solution becomes more difficult, resulting in the formation of more aggressive crevice solution. Crevice corrosion starts close to the crevice mouth and becomes more widespread, moving to the interior of the material throughout the period of exposure to the aggressive solution. As in the case of pitting, crevice corrosion is initiated only above a certain electrode potential. Crevice corrosion has three stages: incubation, initiation, and propagation. The duration of each stage depends on geometric, metallurgical and environmental conditions and therefore the duration of the steps can vary significantly. Though crevice corrosion is widely studied, still little understanding exists on the processes that occur during the onset of stainless steel crevice corrosion (e.g. mechanism of passive film formation and breakdown in stainless steel alloys). Several researchers found either pits or metastable pits in the initial stage of crevice corrosion of stainless steels. Recently, initiation of crevice corrosion has been related to metastable pitting within the crevices, showing that the initiation of these two types of corrosion in iron- and nickel-base alloys is practically the same. An example of crevice corrosion principle is shown in Fig. 6. [1,3,13,14,16-18]

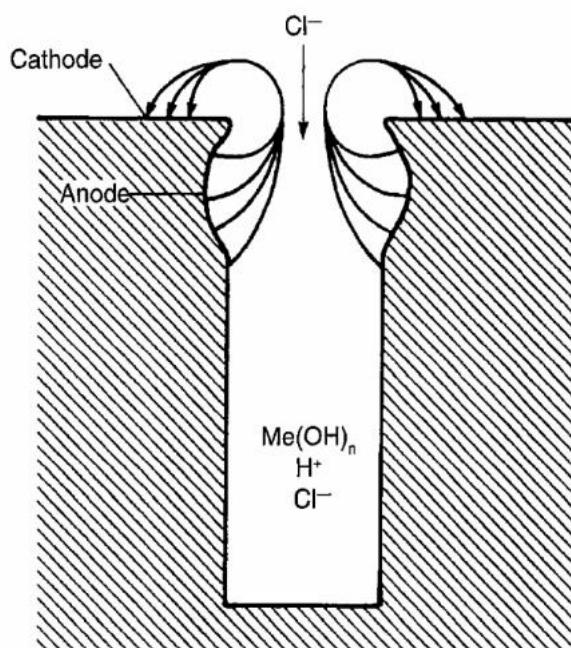


Figure 6. The principle of crevice corrosion. [3]

2.4 Factors affecting crevice corrosion

There are several factors that are responsible for crevice corrosion initiation in stainless steel alloys [14]. These parameters need to be considered when modelling of crevice corrosion is of interest. The main factors and their combined effect on crevice corrosion are studied in the next chapters. Factors affecting passivity and pitting was already mentioned in the Chapter 2.1 and 2.2., so some same issues (as the effect of oxide films, repassivation, acidity, and temperature) are shortly mentioned also here.

2.4.1 Oxide films

Almost all passive films have multilayer structures, usually with the inner oxide and the outer hydroxide layer. The oxide layer is a barrier against cation transfer, and on the hydroxide layer the exchange with the electrolyte takes place. The resistance of stainless steels to localized corrosion is a function of the thickness and composition of the passive film on the metal surface. Stainless steels exhibit an oxide film usually 1-5 nm thick which provides resistance to localized corrosion on the metal surface. The stability of passive film formed on austenitic stainless steels is dependent on alloy composition, temperature, and the exposed environment (Chapter 2.1.). For example the presence of chromium and molybdenum in the oxide increases crevice corrosion resistance of stainless steel alloys (see next chapter). The corrosion initiation usually begins at the potential where the breakdown of the passive film occurs. [5,14,19]

When the effect of oxide films to crevice corrosion is studied, the transport of different metallic constituents, matter and charge through the film must be considered. The interaction between the film and the environment can include many different reactions e.g. adsorption, surface complex formation and re-precipitation of various cations at different pH levels and locations of the oxide film. Oxide penetration and thinning mechanisms also should be considered. [5,14,20]

2.4.2 Alloying elements in metals

The presence or absence of certain alloying elements in stainless steel results in higher or lower crevice corrosion initiation and propagation resistance, and the influence of these elements vary with temperature and pH. Stainless steels containing relatively high levels of molybdenum, nickel and chromium (elements which are known to increase resistance to depassivation) are less prone to localized corrosion. The beneficial effect of chromium and nickel ions is based on stabilization of passive film by shifting the corrosion potential (during crevice corrosion initiation) or the critical crevice potential into the noble direction. Therefore usually stainless steels that have high molybdenum, nickel and chromium levels require very low pH and high chloride ion concentration to cause a breakdown of their passive film. Also copper ions and the synergistic action of nitrogen and molybdenum in stainless steels increase the resistance of alloys to passive film breakdown. Detrimental effect on the corrosion resistance of metals shows elements such as sulphur and manganese. [14,19]

Also other metal structure related factors as alloying elements affect the crevice corrosion sensitivity. Examples of these are second-phase particles, solute segregated grain boundaries, flaws, cold work and the degree of surface roughness. The locations of these factors implicate which areas are sensitive to localized corrosion initiation. Microstructure of a metal or an alloy and its processing route mainly control the formation and sites of the factors mentioned above. [5]

2.4.3 Repassivation

Under certain circumstances, the increasing corrosion partial current that follows a nucleation of a corroding pit may cease. While the repassivation of the corroding surface decreases the growth of pits, the increasing Ohmic potential drop along the depth of the pit also results in

the pit being stable at a low anodic current density at the bottom. This is because, as the pit deepens, the diffusion of the cations out of the pit reduces, thus decreasing the rate at which these ions dissolve from the substrate. At some point, the pit stops growing and is considered 'dead'. It is necessary to determine whether the presence of different phases or other microstructural features in the local neighbourhood would have any influence on whether a pit repassivates or not. Repassivation kinetics is considered critical in determining the localized corrosion resistance of metals and alloys, and in influencing the accumulated damage. [5]

2.4.4 Geometry

Crevice geometry has great influence to crevice corrosion sensitivity. Increasing the crevice tightness and depth the chances for crevice corrosion initiation increase. The width and depth of the crevice control the access of oxygen into the crevice and affect the internal gradients of concentration, potential distribution, etc. Not every crevice existing on the metal structure suffers of localized corrosion. There are certain optimum crevice widths at which the given material is resistant to crevice corrosion. In sufficiently wide crevices, the access of oxygen and the exchange with the external solution is not significantly affected. In very narrow crevices, on the other hand, the concentration gradients are so steep that the breakdown of passivity can occur even close to the mouth of the crevice. In this case, deeper regions will be free of a corrosion attack. However, a wider gap creates smaller IR drop in the crevice electrolyte than a tighter gap, thus resulting in more chances of crevice corrosion initiation. Also in some cases deep crevices may restrict propagation because of a voltage drop through the crevice solution. The use of higher-alloy stainless-type material offers the advantage of providing resistance over a broader range of conditions. [1,13,14]

Most practical crevices have crevice gaps on the order of 0.1-10 mm, and lengths of 1-10 mm. To simplify calculations and modelling it is usually assumed that crevices have ideal dimensions; perfectly vertical side walls and uniform crevice gaps. Practical crevices and crevices fabricated for experiments by pressing two pieces of material together, however, do not have ideal dimensions. It has been reported that sub-crevices created by irregular crevice wall morphology have a significant impact on the ion concentration distributions inside a crevice, and that these sub-crevices dominate the crevice corrosion behaviour of stainless steel type 304 and titanium alloy 825. It has also been proposed that for a crevice depth of 0.1 cm, a gap of less than 0.01 μm might be required for initiation of crevice corrosion of type 304 stainless steel in natural water with 1000 mg/l chloride ion content. [14,21]

2.4.5 Temperature, pH and chemical environment

During the corrosion process, increase in temperature accelerates the reaction kinetics of metal dissolution and related reduction reactions causing the breakdown of the passive region. An increase in temperature causes higher conductivity of electrolytes thus leading to a corresponding increase in the rate of electrochemical reaction and anodic current. However few studies have indicated that for AISI 304 and 316 stainless steels immersed in naturally aerated seawater for 28 days at 10, 25 and 50°C, it was observed that corrosion was more severe at 25°C than at 10 or 50°C. Reason for this "unusual" behaviour could be that at a higher temperature of 50°C, oxygen solubility is reduced, which decreases the external cathodic reaction rate, and in the end lowers the corrosion rate.

The acidity or the alkalinity of the corrosion environment significantly affects the corrosion behaviour of metals in many ways. In the case of crevice corrosion the migration of anionic species (e.g. Cl_2) from the bulk solution to the crevice to preserve electro-neutrality and the hydrolysis of the dissolved metal ions lowers the pH in the crevice solution. This acidification and chloride build-up in the crevice during active stages of crevice corrosion is aggressive to most metals and tends to prevent repassivation and promote corrosion. Also the bulk environment chloride levels and acidity affect the crevice electrolyte pH and chloride level.

Corrosion inhibitors in the electrolyte have the opposite effect to crevice corrosion, since they slow down the corrosion reactions. The availability of redox species is an important factor in crevice corrosion, since it controls the rate of reduction and dissolution reactions. More about the reactions taking place in crevice corrosion is found in Chapter 3.2. [5,14]

During localized corrosion, some salts precipitate on the corroding substrate as a result of reactions between dissolved anions and species in the electrolyte in the pit or crevice. Precipitation occurs when the product of the ionic reactants exceeds the solubility product. The corrosive microenvironment under surface deposits is very different from the bulk solution, e.g. pH of these microenvironments tends to be very acidic. [5]

Fig. 7 shows schematically how few of the parameters mentioned above might affect corrosion sensitivity. The critical chloride condition for localized corrosion to occur is when repassivation potential E_{rp} is lower than corrosion potential E_{corr} (Fig. 7a). Similarly, for a given chloride concentration a critical temperature (Fig. 7b) and a critical inhibitor concentration exist (Fig. 7c). In many processes, incidental contamination of the process fluid by redox species may increase the E_{corr} such that localized corrosion may occur beyond a critical concentration of redox species. The actual condition in a system may be a combination of the idealised cases shown in Fig. 7 a–d. [7,22]

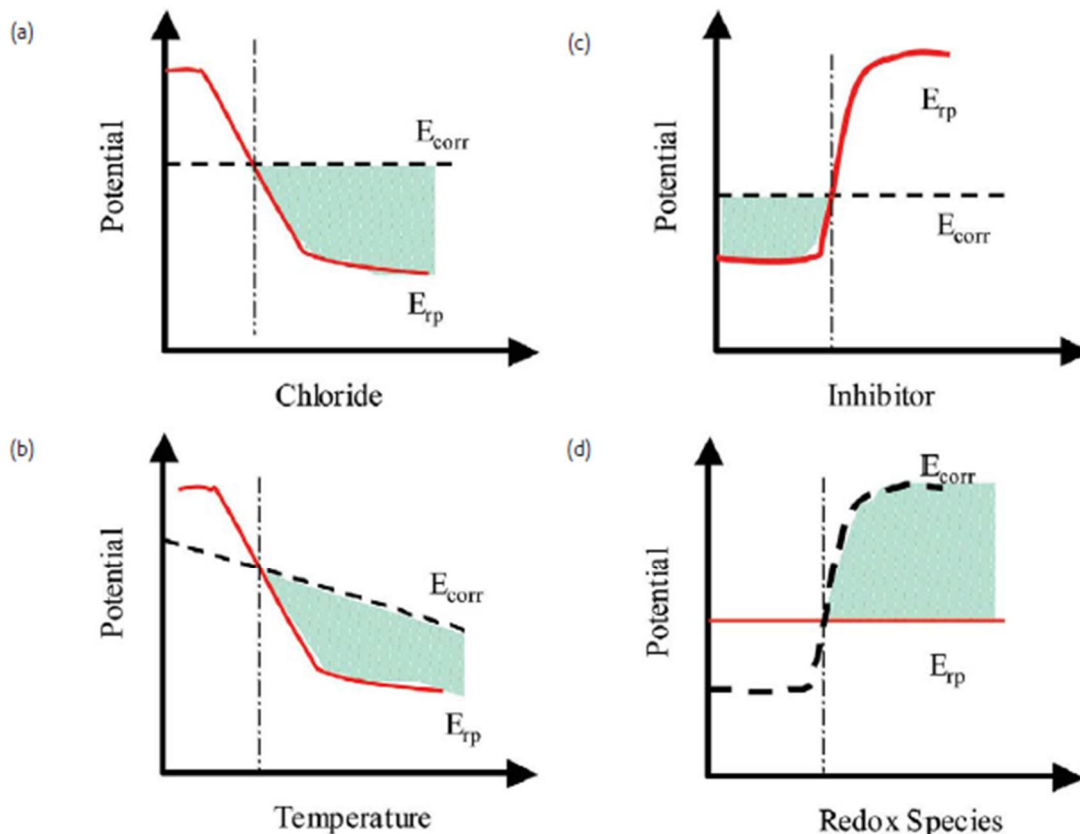


Figure 7. Schematic diagram of the effect of Cl^- (a), temperature (b), inhibitors (c), and oxidizing redox species (d) on the relative values of E_{rp} and E_{corr} . The shaded areas denote the ranges in which localized corrosion can be expected.[7]

2.5 Theories of crevice corrosion

2.5.1 Critical IR Drop theory (IRDT)

Critical Potential IR Drop theory as well as critical crevice solution theory (next chapter) describes the processes occurring during crevice incubation which determine the possibility of crevice initiation. Both theories are based on the idea that the crevice former acts as a

barrier to electrical current. The IR mechanism (I indicates the current within the crevice electrolyte and R the resistance of the electrolyte) of crevice corrosion development predict the presence of the most severe attack at the area between the pit bottom and the crevice mouth and explain the crevice corrosion in the systems where acidification does not occur but an active/passive condition exist on the crevice walls. For crevice corrosion initiation by the IRDT an aggressive local chemistry is required within the crevice, hence, this theory does not apply to the passive metals which do not exhibit active/passive behaviour and drop of the potential in the crevice is very low. [1,18,23]

The IRDT includes three steps. During the first step a separation of anodic and cathodic sites, caused by oxygen depletion inside the crevice or anodic polarization of the entire surface by another electrode, takes place. Until this occurs there is no net current flowing from any surface since the anodic and cathodic reactions are everywhere equal. In the second step anodic current flows from the crevice to balance the charge flow, which results in a potential difference (the third step). During the third step the net current flow over the electrically resistive solution causes potential difference between the crevice and the cathodic sites on the exposed surface. The effect of this resulting potential difference depends on the nature of the polarization curve for the material/environment system. For an active/passive metal, that is held in its passive region the effects of potential drop can be devastating. The critical amount of potential drop which must occur to initiate crevice corrosion is the difference between the potential at the mouth and the Flade potential i.e., passivation potential. Fig. 8 shows the effect of the IR drop on reaction kinetics. In Fig. 8, the cathodic polarization curve is shown without any IR effects. This curve only cuts the anodic polarization curve within the passive region, resulting in a very low corrosion current (i.e., very low corrosion rate). The cathodic polarization curve with IR effects is shown to cut the anodic polarization curve below the critical potential, in the active region, resulting in significantly greater magnitudes of corrosion current.

The advantages of the IRDT are that it can predict the location and morphology of attack and has been shown to operate in systems where there is no possibility of significant changes in composition. The weaknesses of IRDT are that it cannot rationalize the observed incubation times, and it ignores the effects of the accumulation of chemical products within the crevice. IRDT as well as CCS are for pure metals and ignore the important role of microstructural inhomogeneities (including surface roughness) on corrosion initiation on engineering alloys. [5,18,23]

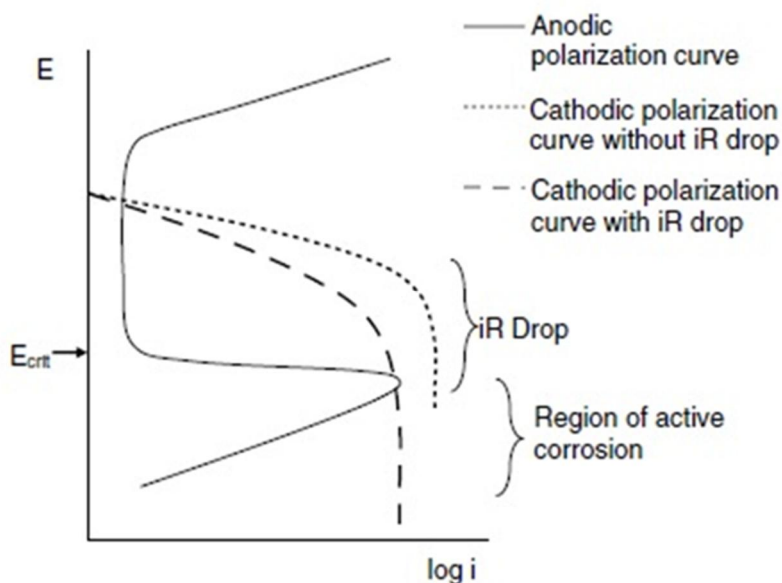


Figure 8. Idealized kinetic corrosion diagram for a passive metal. [18]

Another schematic presentation of IR-type crevice corrosion is shown in Fig. 9. In Fig. 9 IR voltage produces an electrode potential E_x and metal dissolution $i(x)$ distribution (polarization curve) on the crevice walls, and causes migration in and out of the crevice. The factors controlling the location of the passive-to-active transition $E_{A/P}$ on the crevice wall are the critical depth L_c (or critical aspect ratio) for a crevice of depth L and the opening dimension. Crevice corrosion occurs immediately if $E_{A/P}$ exists on the crevice wall, i.e., when $L_c \leq L$. The transition from the passive to the active dissolution on the crevice wall occurs at a certain distance into the crevice, $X_{A/P}$, which is located at the $E_{A/P}$ value on the crevice wall. $\Delta\Phi^*$ is the potential difference between the applied electrode potential in the passive region ($E_{app} = E_x = 0$ at the crevice opening $x = 0$). [1,24]

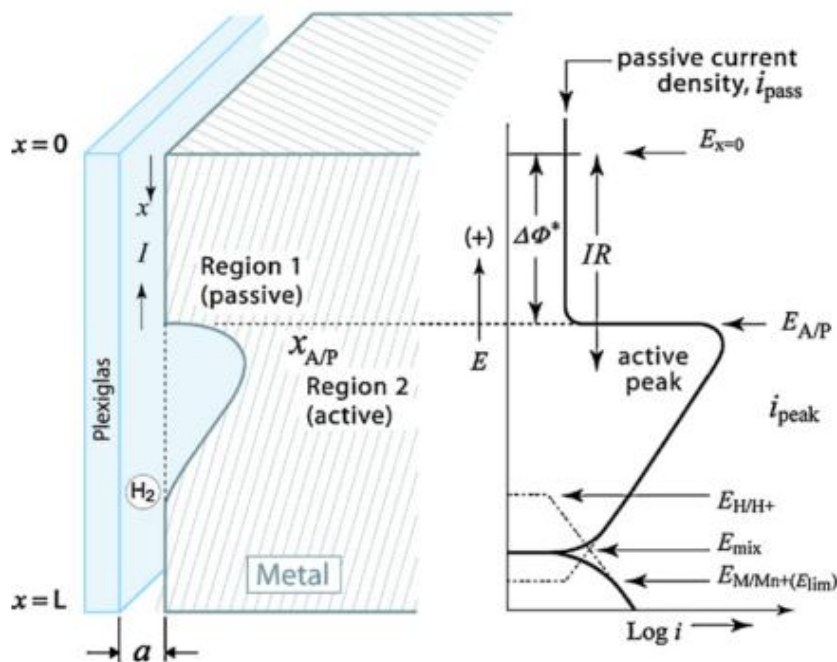


Figure 9. Schematic illustration of the crevice corrosion cell and the IR-produced $E(x)$ and resulting $i(x)$ current density distribution (polarization curve) on the crevice wall. Metal is passive above the $x_{A/P}$ boundary and active below it, for a crevice whose only opening to the bulk electrolyte is on the top surface. [24]

2.5.2 Critical crevice solution (CCS) theory

Critical Crevice Solution (CCS) theory is based on the idea that slowly diffusing metal cations attract chloride ions into the crevice to form a hydrochloric acid solution, which causes disruption of the passive film, when the crevice corrosion will initiate. The process feeds on itself and destroys the underlying substrate. In Fig. 10 an idealized corroding crevice is presented.

CCS theory consists of four steps, from which the first step includes deoxygenation. The free oxygen within the occluded site is consumed, since any O_2 diffusing down the long diffusion path of the occluded site is consumed near the mouth. Then cathodic reactions support the dissolution to occur outside the crevice, because it is easier to move electrons through the metal substrate than ions through solution. The second step includes hydrolysis: metal cations form metal hydroxides which lowers the pH value due to the release of H^+ . Metal cations accumulate because of the large diffusion path from crevice depths to bulk environment. In the third step only anodic reactions are occurring in the crevice, since positively charged metal cations (e.g. Fe^{2+} , Cr^{3+} , Ni^{2+}) are transferred into the solution. Chloride ions will flow into the crevice to balance the positive charge. Chloride destabilizes

the passive film, acting along with the increased acidity to increase the corrosion rate. In the fourth step the acid generation by metal hydrolysis and rise in chloride levels raises the corrosion rate. This leads to further propagation of the hydrolysis reaction and, in parallel, further increased chloride levels, and the process proceeds in an autocatalytic manner.

CCS theory's advantages are that it explains the relative sensitivity of various stainless steel grades to crevice corrosion and accounts for the initiation time. The main problem with the CCS theory is that it ignores the effects of potential on crevice corrosion, yet potential has a large effect on reaction rate. [18,23]

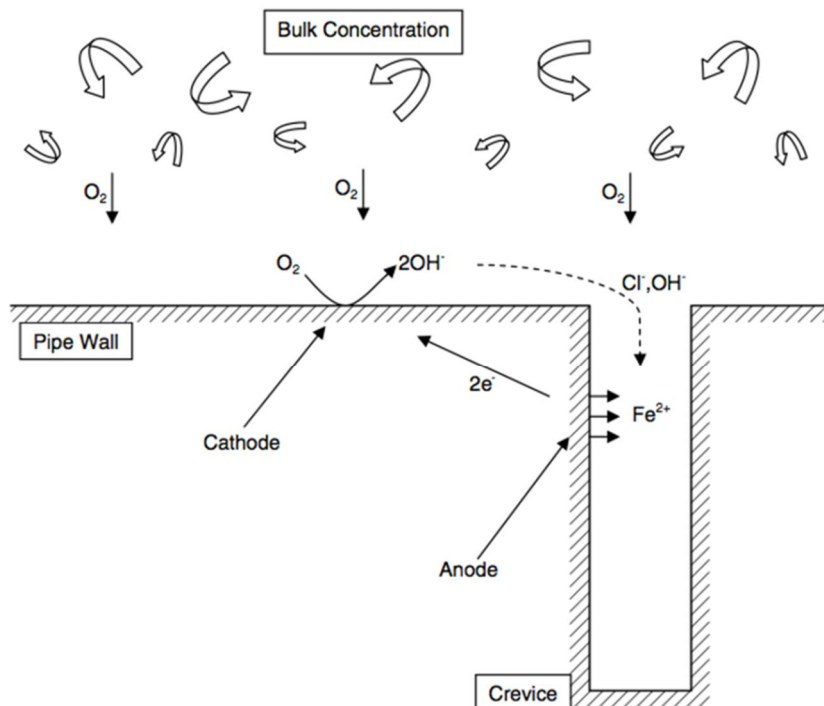


Figure 10. Idealized corroding crevice. [18]

2.5.3 Coupled environment theory

The mechanisms of localized corrosion are usually understood by the idea of the local anode within the crevice and the local cathode on the external surface, which are the locations that have the least and greatest access to the cathodic depolarizer O_2 . To compensate the accumulation of positive charges (metal cations and H^+ , the latter of which results from metal cation hydrolysis) in the crevice, anions (commonly Cl^- and OH^-) are transported from the bulk electrolyte into the crevice. This results in a positive current flowing through the metal in the same direction. The positive and negative currents annihilate each other at the external surface via "charge transfer reaction" such as reduction of oxygen or evolution of hydrogen, Fig. 11. This type of mechanism is termed a coupled environment (crevice) theory as it describes the strong electrochemical coupling between the crevice and the external surfaces which results in a flow of "coupling current" between the crevice and the outer surfaces. Coupling current indicates crevice activity and provides information on the processes taking place inside the crevice. Two important factors have been detected for the coupled environment theory by Lee et al. [25] via experimental and theoretical work: 1) localized (crevice) corrosion can be stopped or prevented by ensuring that the coupling current becomes zero, and 2) kinetics of the reactions on the external surface affect the controlling of the coupling current and hence the rate of damage accumulation within the crevice. Example of the first factor is that, if the external surfaces are coated with a layer of electrically insulating material, such as ZrO_2 , the exchange current density for oxygen reduction is so

small that coupling current becomes zero (also absorbed inhibitors can create such an insulating coating). Numerous studies show that tight crevices quickly deplete of cathodic depolarizers (such as O_2) and that the fraction of coupling current that is consumed on the crevice walls compared to that which flows to the external surface, is small and insignificant. However the authors of this theory claim that the build-up of H^+ within the crevice via hydrolysis of metal cations may occur to the extent that the reduction of protons within the crevice becomes the principal cathodic reaction in the system, resulting in crevice inversion (anodic reaction moves to the external surface). [25]

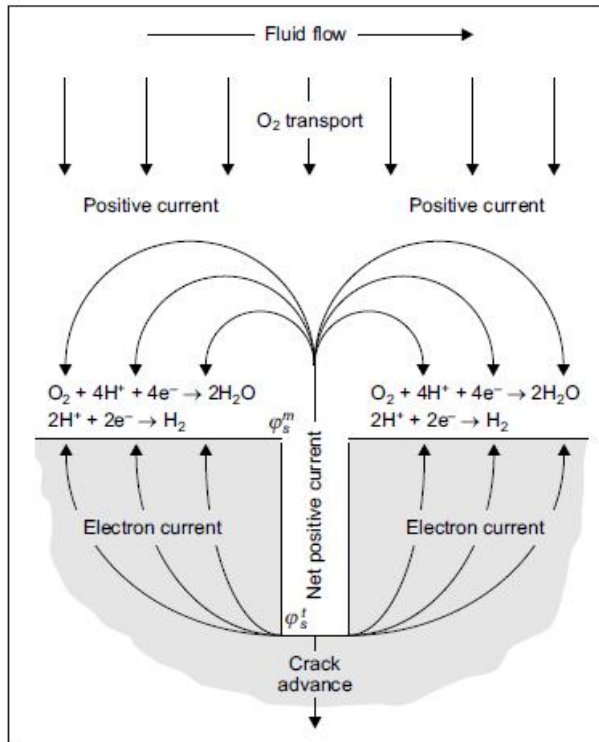


Figure 11. Coupling of crack internal and external environments. At steady state, the crack can grow as fast as the positive current flowing from the crack can be consumed on the external surfaces by oxygen reduction. ϕ_s^m and ϕ_s^t are the electrostatic potentials in the solution with respect to a reference electrode or metal. [25]

2.5.4 Repassivation potential approach

Anderko et al. [22] have developed a different approach to localized corrosion by focusing on the repassivation potential E_{rp} . The approach divides study of localized corrosion into two independent parts: predicting the E_{rp} for localized corrosion and the corrosion potential E_{corr} . The idea in the use of E_{rp} is the fact that for engineering applications, only the behaviour of stable pits on crevice corrosion is important. Pits that nucleate, but do not grow beyond a specific stage (metastable pits) do not have a detrimental effect on the performance of engineering structures. It has been shown before that the E_{rp} is the potential below which crevice corrosion does not occur, and it is relatively insensitive to pit depth and surface finish. E_{rp} is lower than the breakdown potential and therefore a more conservative value to use as a design parameter. The separation of the problem into two parts involving E_{rp} and E_{corr} is valid, because E_{corr} is not affected by localized corrosion at the early stages where the area of the actively corroding pit is insignificant compared to the overall area. Localized corrosion can happen when the E_{corr} is higher than the E_{rp} , and is unlikely to happen if the E_{corr} is lower than the E_{rp} (by a margin of 100 mV or more). An example illustrating the relationship between E_{rp} and E_{corr} can be seen in Fig. 7 (Chapter 2.4.5). One option is to compare the predicted E_{rp} to the E_{corr} using the mixed potential theory (Chapter 3.2.2). [7,22]

2.5.5 Metastable pitting theory

Measurements of crevice solution chemistry suggest that, rather than a gradual change of local chemistry causing crevice corrosion, the sudden initiation of crevice corrosion causes a sudden change in the local chemistry. Stockert et al. [26] proposed a theory based on the idea that crevice corrosion is simply a geometrically stabilised form of pitting. Metastable pits are stabilised by the presence of a porous pit cover which provides an ohmic drop sufficient to keep the pit bottom in the active state, or acts as a diffusion barrier helping to maintain a concentrated local chemistry. If the local chemistry changed, the metastable pit would die through repassivation. However, they suggested that if a metastable pit formed within a crevice and its cover would broke, the resistive barrier of the crevice geometry was sufficient to stabilise the pit. The nearby area of the crevice would then be exposed to the aggressive pit environment and general breakdown could proceed. On an open surface, such pits must usually precipitate a salt film in order to survive the eventual collapse of the pit cover. Also Jakobsen et al. [9] concluded in their study of AISI 316 stainless steel that crevice corrosion shows pointwise initiation at temperatures in and above the transition interval, and the initiation seems to happen by geometrical stabilization of metastable pits. Currently, many authors support the conception of crevice corrosion evolution from the metastable pits formed within the crevice. When the covers on the metastable pits rupture, the pits' solution will spread and mix with the crevice solution, leading to acidification of the crevice solution. It needs to be noted that this mechanism will apply only to crevice corrosion on passive metals and on alloys (e.g., stainless steels) which undergo pitting in chloride solutions. [1]

3 Crevice corrosion modelling

When the goal is to find the best modelling solution for various metal-environment combinations, a review on previous modelling attempts of the subject is essential. As it was mentioned in the previously, a model that can describe all the factors affecting crevice corrosion is at the moment considered too challenging, so the modelling solutions are mainly compromises between selected perspectives. The published models have a number of similarities in simplifying assumptions because of the difficulty in modelling of different systems. [4]

Sharland et al. [6] investigated common problems of different pitting and crevice corrosion models. They concluded that mathematical models may be broadly divided into two categories: mechanistic models and empirical data-fitting models. Also the third category of statistical models exists. Models which neglect ionic diffusion under concentration gradients are only valid at short times since any build up in potential means some imbalance in ionic concentrations and following diffusion. The models that neglect migration under potential gradients are also quite restricted in their applicability, since they are either specific to some experimental system in which the potential gradients have been shown to be small over the relevant time scales or they consider only the transport of neutral species. Several models indicate ranges of certain parameters in which each transport process dominates. The more general models are those which consider diffusion and electromigration. The used models are usually divided into analytical and numerical models. The analytical models provide a clearer assessment of the effects of the various physical processes, for example the influence of crevice geometry. The general numerical models usually relate more to engineering needs, for example materials selection. [6,27]

In the next chapters the general structures and challenges in modelling (especially from the multiscale modelling point of view) as well as the chemical reactions and equations valid for crevice corrosion modelling are being studied. The performed experiments, and existing models for crevice corrosion of different research teams are reviewed. The suitability, advantages and disadvantages, of different models for certain metal-environment systems is also determined. Both empirical and mathematical models are included.

3.1 Structure and challenges of crevice corrosion modelling

Traditional approaches for modelling localized corrosion are usually based on 1) the E-pH or Pourbaix diagrams (thermodynamics), 2) the polarization or Evans diagrams (kinetics) or 3) the Nernst–Planck equation and the transport models that are based on the concentration solution theory. These methods provide integral information on the electrochemical processes that occur at the solid/liquid interfaces. Information on local atomistic events and the influence of surface imperfections on the interfacial processes are yet on the level of development. [5]

The available single-scale corrosion models may be divided into various categories (Table 1), based on the predictions about the characteristics of corrosion events (deterministic or statistical) and the scales involved (atomic or continuum). Today the deterministic models generally focus on the growth of a single, previously established pit (or crevice) or a collection of pits with predetermined anodic and cathodic sites. However, these models do not include pit initiation events because the currently available experimental knowledge is insufficient to model deterministically atomic scale events like pit initiation, which is difficult to observe physically. Some researchers have tried to combine elements of deterministic and statistical models to minimize the limitations of the two approaches. For example, Laycock et al. [28] developed an experimentally validated hybrid model for pitting and crevice corrosion, where a purely statistical model for pit initiation was combined with a deterministic model to propagate single pits in stainless steel. An ideal corrosion model would include a multi-scale model (MSM), which could link the atomic and continuum scale behaviour together. For example, in a potential MSM an atomistic model may be embedded within a mesoscopic model, which can be embedded within a continuum scale model. Then, the lower-scale model can update the higher-scale model at regular time intervals with the corrosion damage information. Many models include finite element method (FEM) as a basic tool. However, also meshless methods for modelling exist. These methods are better suited to tackle the moving discontinuities, such as random crack propagation and complex paths, whereas the traditional FEM methods would involve considerable meshing and re-meshing. [5]

In literature, mesoscopic scale CA (cellular automaton) models were mentioned, because CA models are among the few methods that account for global charge conservation, which is a major requirement for corrosion. The CA models can be refined to an atomistic level and the atomistic-mesoscopic scale coupling can be achieved by refining the cells to match the atomistic surface morphology. This refinement could place a high computational load on the current CA models especially for corrosion on an adjacent metal surface. The CA models could be combined with control-volume finite element method (CVFEM), which will account for reactions and ionic movement in the solution phase. Additionally, smoothed particle hydrodynamics (SPH) is another method that can include localized precipitation. [5,14]

Table 1. Types of single-scale models that relate to localized corrosion. Categorized based on the assumptions relating to characteristics of events modelled.[5]

Main category	Sub category	Description
Deterministic	Atomic scale	Quantum mechanics (QM) calculations are performed at the atomic level, Molecular Dynamics (MD) calculations are performed at the atomic scale
	Continuum scale	Partial differential equations (PDEs) are solved using one of the following methods: analytical, finite element method (FEM), finite difference method (FDM), boundary element method (BEM) or finite volume method (FVM)
	Cellular automaton (CA) models	In the CA models, the new state of a cell is a function of all states in the cell's neighbourhood at the previous moment in time. Most CA models follow deterministic rules to update the cell states (although the choice of the deterministic rule itself can be randomised)
Statistical	Atomic scale	A Monte Carlo (MC) model that incorporates statistical variability for the pit initiation and the pit widths
	Continuum using probability density functions (PDFs)	PDFs describe the likelihood that a pit would initiate at a given location at a given time under given conditions; PDFs are also applied in some cases for the pitting frequency, the pit incubation time and the pit generation rate
	Continuum using artificial neural networks (ANNs)	The relationships between the causal parameters and the observed effects are developed without a deep knowledge of the physics; ANNs are criticised for their 'black box' nature, greater computational burden, etc.
Hybrid	Continuum scale	Elements of the deterministic models are combined with those of the statistical models

When creating a MSM model, we first need to decide whether the model requires a two-scale or a three-scale model (meso/continuum scales) approach. One important matter in the modelling is to consider the solving of equations on different scales: there is a big difference in characteristic time scales between (a) the almost instantaneous phenomena such as electromigration, chemical reactions and electrochemical reactions; and (b) the slow processes such as diffusion. A realistic MSM for the development of corrosion-resistant alloys and inhibitors should be coupled to an MSM on alloy solidification. An MSM on microstructure prediction should ideally be linked to an MSM on localized corrosion, so that through a feedback loop, the alloy system may be optimised for corrosion performance. [5]

A general description of a potential MSM on localized corrosion is presented in Fig. 12. Factors mentioned in Fig. 12 were discussed in more detail in Chapters 2.1- 2.4 and 3.2. Few common challenges that include developing an MSM are listed below:

- The overall formulation of the model so that processes and structures are modelled on appropriate scales
- The development of models at each scale that are computationally efficient and provide results of appropriate accuracy and resolution
- The linking of models on different scales in a computationally efficient manner
- The validation of the model overall and at each level.

The exact method to link different scales probably will depend on the particular material and processes involved, and thus a tool-box rather than a prescriptive approach may be best. The amount of the requirements for ideal crevice corrosion model is obviously very large,

and it is rather difficult for a single model to meet all the challenges. Therefore the existing models usually consist of simplified systems, which consider specific reactions, equations and environments. [5]

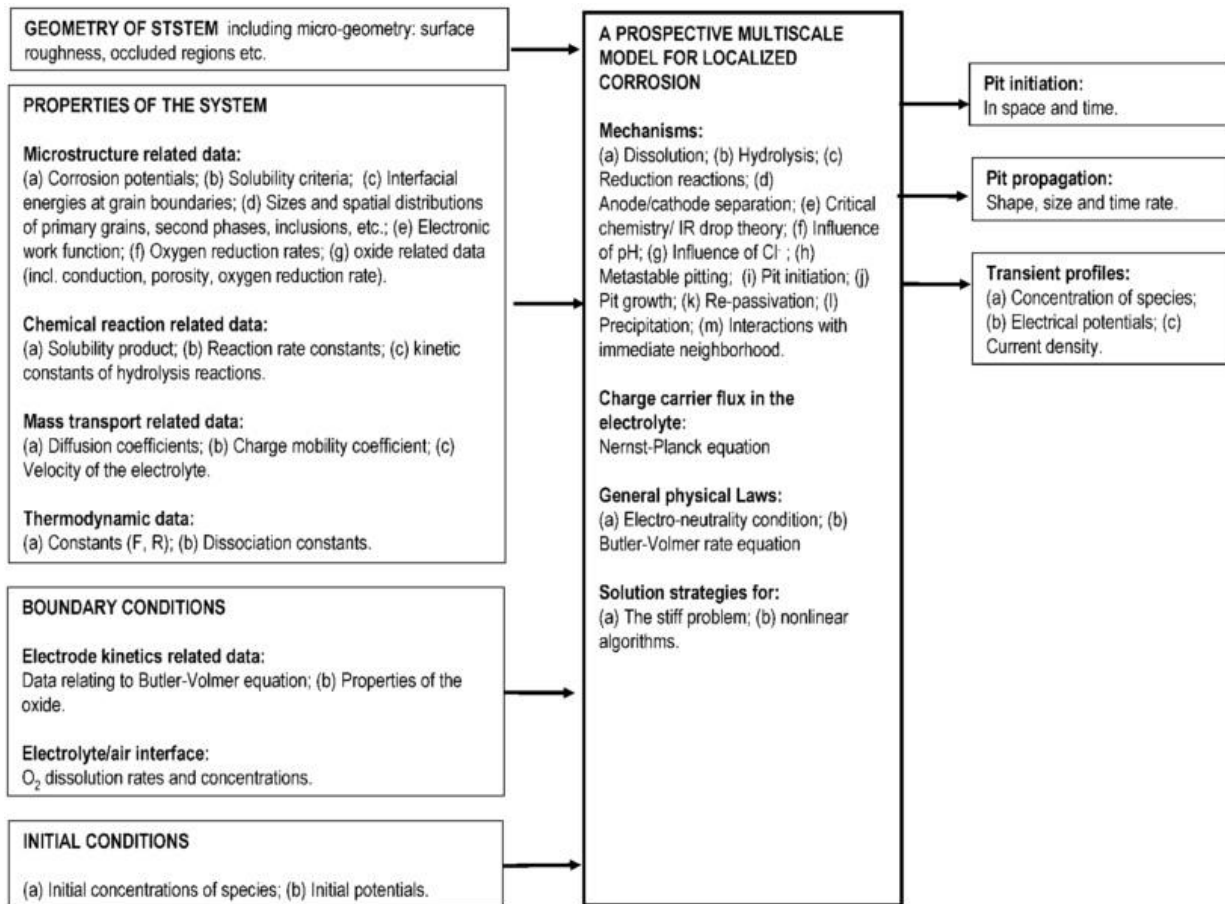


Figure 12. General description of a prospective multiscale model (MSM) on localized corrosion including potential inputs and outputs. [5]

3.2 Relevant electrochemical reactions and equations in crevice corrosion modelling

To be able to describe the corrosion processes in the crevice environment, the actual electrochemical reactions of different species are needed. The main reactions that need to be considered for the modelling are relevant hydrolysis, transport, and redox reactions. Understanding on the kinetics of all of these reactions is necessary when the reaction and corrosion rates are to be evaluated. The reactions taking place during crevice corrosion initiation and propagation can differ from each other, and proceed at various rates. Also the relevant equations for crevice corrosion are mentioned. The studied reactions and equations exist in large amounts, and not all of these are mentioned here. Mainly the most general and frequently used formulas are being presented.

3.2.1 Electrochemical reactions

When developing a crevice corrosion model, the following reactions must be considered:

- Metal oxidation
- Metal ion dissolution, diffusion, speciation and hydrolysis
- Reduction of oxygen, and other species

- OH-ion dissolution, diffusion and further solution reactions
- Precipitation of corrosion products from the solution
- Effect of initial oxide layer
- Solution chemistry (migration and diffusion of other species like Cl_2 and inhibitors)

In Table 2 few common ions important in crevice corrosion and their diffusion coefficients are presented. The higher the diffusion coefficient (of one substance with respect to another), the faster they diffuse into each other. Diffusion coefficients in gases are of the order of $10^{-5} \text{ m}^2/\text{s}$, those in solutions the order of $10^{-9} \text{ m}^2/\text{s}$, and in solids the order of $10^{-14} \text{ m}^2/\text{s}$. The concentrations of these ions naturally depend on the electrochemical reactions taking place and on the overall system chemistry (Table 2). [5,16,29,30]

In Table 3 the reduction reactions 1 - 9 are relevant for crevice corrosion initiation. During crevice corrosion initiation (when considering metallic crevice and oxygen-saturated electrolytic solution at neutral pH) metal dissolution (Table 3, reaction 10) and the accompanying cathodic oxygen reduction to hydroxide ions (Table 3, reaction 2) occur uniformly over the metal surface, also inside crevice. During crevice corrosion propagation when oxygen differential cell is created, the hydrolysis of metal ions (Table 3, reaction 11) takes place along with the hydrolysis of products and precipitation of hydroxide (Table 3 reaction 12). Factor that can affect the crevice corrosion propagation is the possible formation of solid metal salts on the surfaces when dissolving cations and Cl_2 ions combine and reach saturation concentration of the salt. The formation of deposits on pits usually limits diffusion at pit mouths, and thus help to maintain the critical chemistry in the pits. M in the reactions 10-12 and 14 represents a metal in general and n is the valence of the metal. The n naturally varies according to the metal involved. The reaction 12 limits the concentrations of metal species in the oxide film and in the crevice via precipitation. The reactions 14 are examples of additional reactions occurring in chloride concentrated environments. An example of the reactions occurring in crevice corrosion is presented in Fig. 13 for AISI 304 stainless steel in NaCl solution. [4,5,14,16,27,31,32]

Table 2. List of few common ions and their diffusion coefficients (at $T=298.15 \text{ K}$) to be considered in crevice corrosion. [16,29]

Ions	Diffusion coefficient (m^2/s)
Cl^-	2.0×10^{-9}
H^+	9.3×10^{-9}
H_2	4.4×10^{-9}
OH^-	5.2×10^{-9}
O_2	2.0×10^{-9}
H_2O_2	2.0×10^{-10}
SO_4^{2-}	1.0×10^{-9}
HSO_4^-	1.4×10^{-9}
CO_3^{2-}	9.8×10^{-10}
HCO_3^-	1.2×10^{-9}
Na^+	1.3×10^{-9}
$\text{Fe}(\text{OH})^+$	7.1×10^{-10}
Fe^{2+}	7.1×10^{-10}
$\text{Ni}(\text{OH})^+$	7.0×10^{-10}
Ni^{2+}	7.0×10^{-10}
$\text{Cr}(\text{OH})^{2+}$	6.0×10^{-10}
Cr^{3+}	6.0×10^{-10}

Table 3. The few relevant reactions required for crevice corrosion modelling and their corresponding equilibrium potentials. P_x refers to partial pressures of gaseous species X, (often assumed to be 1 atm) [4, 14, 16, 29, 31, 32]

Type	Reaction	Equilibrium potential (V_{SHE}) $T=25^\circ\text{C}$	Reference
1. Reduction of Oxygen (acidic conditions)	$\text{O}_2 + 4\text{H}^+ + 4\text{e}^- \rightarrow 2\text{H}_2\text{O}$	$E = 1.228 - 0.0591\text{pH} + 0.0148 \log P_{\text{O}_2}$	[14]
2. Reduction of Oxygen (neutral/alkaline conditions)	$\text{O}_2 + 2\text{H}_2\text{O} + 4\text{e}^- \rightarrow 4\text{OH}^-$	$E = 0.401 + 0.0148 \log P_{\text{O}_2} - 0.0591 \log [\text{OH}^-]$	[14]
3. Reduction of Hydrogen (neutral/alkaline conditions)	$2\text{H}_2\text{O} + 2\text{e}^- \rightarrow \text{H}_2 + 2\text{OH}^-$	$E = -0.828 - 0.0591 \log [\text{OH}^-] - 0.0295 \log P_{\text{H}_2}$	[14]
4. Reduction of Hydrogen (acidic conditions)	$2\text{H}^+ + 2\text{e}^- \rightarrow \text{H}_2$	$E = 0.000 - 0.0591 \text{pH} - 0.0295 \log P_{\text{H}_2}$	[32]
5. Reduction of chlorine	$\text{Cl}_2 + 2\text{e}^- \rightarrow 2\text{Cl}^-$	$E = 1.358 + 0.0295 \log P_{\text{Cl}_2} - 0.0591 \log [\text{Cl}^-]$	[32]
6. Reduction of hypochlorous acid (near neutral conditions)	$\text{HClO} + \text{H}^+ + 2\text{e}^- \rightarrow \text{H}_2\text{O} + \text{Cl}^-$	$E = 1.494 - 0.0295 \text{pH} + 0.0295 \log [\text{HClO}] - 0.0295 \log [\text{Cl}^-]$	[32]
7. Reduction of hypochlorite (alkaline conditions)	$\text{ClO}^- + \text{H}_2\text{O} + 2\text{e}^- \rightarrow 2\text{OH}^- + \text{Cl}^-$	$E = 0.890 + 0.0295 \log [\text{ClO}^-] - 0.0591 \log [\text{OH}^-] - 0.0295 \log [\text{Cl}^-]$	[32]
8. Reduction of sulphur	$\text{S} + 2\text{H}^+ + 2\text{e}^- \rightarrow \text{H}_2\text{S}$	$E = 0.141 - 0.0591 \text{pH} - 0.0295 \log P_{\text{H}_2\text{S}}$	[32]
9. Reduction of thiosulphate	$\text{S}_2\text{O}_3^{2-} + 6\text{H}^+ + 4\text{e}^- \rightarrow 2\text{S} + 3\text{H}_2\text{O}$	$E = 0.499 - 0.0887\text{pH} + 0.0148 \log [\text{S}_2\text{O}_3^{2-}]$	[32]
10. Dissolution of metal (at the metal/solution interface)	$\text{M} (\text{s}) \rightarrow \text{M}^{n+} (\text{aq}) + n\text{e}^-$		[16]
11. Hydrolysis of metal ion	$\text{M}^{n+} + \text{H}_2\text{O} \rightarrow \text{M}(\text{OH})^{(n-1)+} + \text{H}^+$		[16]
12. Hydrolysis of product/Precipitation of Hydroxide	$\text{M}(\text{OH})^+ + \text{H}_2\text{O} \rightleftharpoons \text{M}(\text{OH})_2 (\text{s}) + \text{H}^+$		[16]
13. Dissociation of water	$\text{H}_2\text{O} \rightleftharpoons \text{H}^+ + \text{OH}^-$		[16]
14. Additional reactions in chloride exposure	$\text{M}^{2+} + \text{Cl}^- \rightleftharpoons \text{MCl}^+$		[27]
	$\text{MCl}^+ + \text{Cl}^- \rightleftharpoons \text{MCl}_2$		[27]

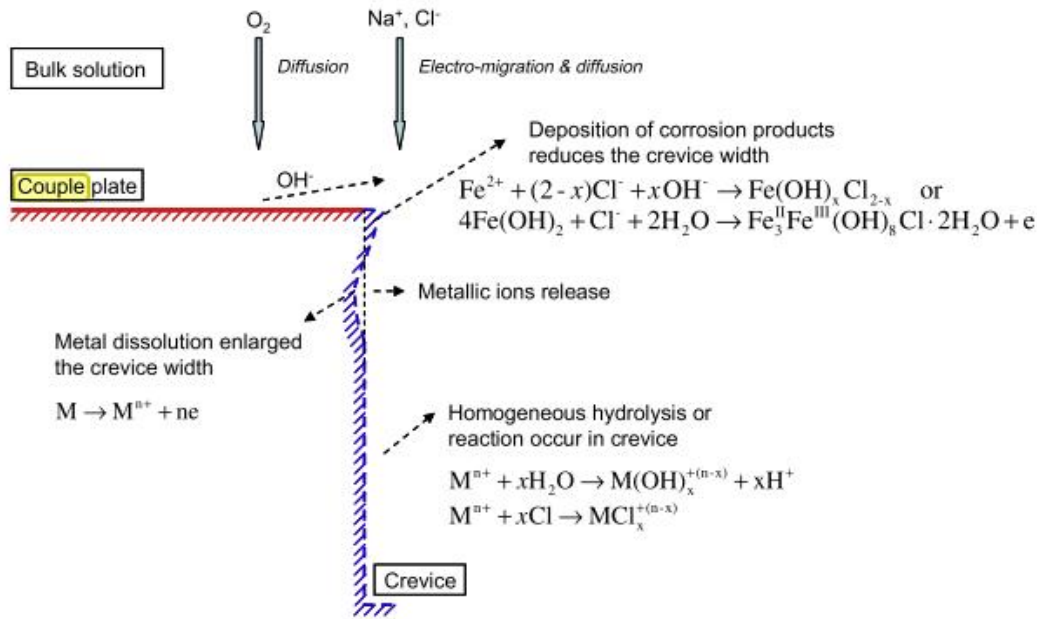


Figure 13. Schematic of the corrosion behaviour of AISI 304 stainless crevice in NaCl solution. [17]

3.2.2 Equations

Chemical and electrochemical equations concerning crevice corrosion need to be defined in order to describe the kinetics of the reactions (e.g. mass transport and corrosion rate) in a satisfactory manner. One common equation used in corrosion models is a statement of charge neutrality in the crevice electrolyte. Charge separations do not occur in real electrochemical systems because observable accumulations of charge produce very large potential differences, and ions would quickly migrate under the resulting electric fields to reduce the excess charge. The charge neutrality can be described as:

$$\sum_i z_i C_i = 0, \quad (1)$$

where z_i is the charge number for species i (eq/mol), and C_i is the concentration of species i (mol/m³). Equation (1) can be used to determine the concentration of one species in order to eliminate any charge differences caused numerically by the application of the chemical transport governing equations to the other species. [23]

Term that is often used, when corrosion or other electrochemical phenomena are being analysed, is mixed potential theory. In the mixed potential theory the potential adopted by an electrode in contact with an aqueous solution containing both oxidizing and reducing species is determined by a balance of the cathodic (reduction) and anodic (oxidation) partial processes occurring at the surface. If the electrode is inert, the resulting potential is known as the redox potential, E_{redox} . If the electrode is electroactive and experiences corrosion, and contributes to the total partial anodic current, the potential is known as E_{corr} (or ECP) of the substrate. Thus, if the partial current densities do not depend on the coordinate on the metal surface, the charge conservation condition for the interface may be written as:

$$\sum_k i_{a,k} + \sum_m i_{c,m} = 0 \quad \text{at } E = E_{corr}, \quad (2)$$

where $i_{a,k}$ and $i_{c,m}$ are partial anodic and cathodic current densities, corresponding to the k th anodic reaction and m th cathodic reaction. This simple theory has proved to have a profound impact on how to interpret the corrosion of metals and alloys in a wide variety of systems. [29]

3.2.2.1 Kinetics

Most electrochemical kinetic models are based on the Butler–Volmer equation, which provides an average free-energy formulation of charge transfer but does not examine the individual processes that are involved in the transfer. Butler-Volmer equation describes the rate of an electrochemical reaction by representing the current density at an electrode in terms of the overpotential. One form of the Butler–Volmer equation is given by Equation (3):

$$i = i_a - i_c = i_0 \left[\exp \frac{(1-\alpha)F\eta}{RT} - \exp \frac{-\alpha F}{RT} \right], \quad (3)$$

where i is the overall current, i_a and i_c are the individual cathode and anode currents (A), and i_0 is the exchange current (A). F is the Faraday constant ($96,487 \text{ C mol}^{-1}$), η is the over potential (V), R is the gas constant, T is the temperature (K), and α is a dimensionless parameter with values between 0 and 1, and is often estimated to be 0.5. [5,33]

Another way to describe the kinetics of a reaction is the Tafel equation. The Equation (4) links the applied overpotential to the current i (A), which passes through the circuit:

$$\eta = \frac{RT}{\alpha F} \ln i_0 - \frac{RT}{\alpha F} \log i. \quad (4)$$

In Equation (4), the y-axis intercept at no over potential can be used to calculate the exchange current, i_0 (A). The usability of Equation (4) is limited by the reverse reaction and diffusion. When the overpotentials are small ($< 50 \text{ mV}$), the slope increases because the backward reaction becomes greater than 1% of the forward reaction, changing the relative concentrations at the electrode surface. When very large overpotentials ($> \text{few hundred mV}$) are applied, the slope of the line can deviate below the prediction of the Tafel equation because of mass-transfer limitations. With the help of Tafel equation the anodic and cathodic currents in a system can be determined [33]. Usually the initiation and early metastable growth phase of a pit or crevice is activation controlled, when Butler–Volmer or Tafel kinetics equations are used. [5]

3.2.2.2 Mass transfer

The mass transfer of a system can be accomplished in three different ways and/or a combination of these modes: 1) migration; movement of charged particles in an electric field, 2) diffusion; movement of species against a concentration gradient, and 3) convection; movement of species induced by stirring or density gradients. The Nernst–Planck equation relates the unidirectional (x) flux of a species j to diffusion, migration, and convection:

$$J_j(x) = -D_j \frac{\partial C_j(x)}{\partial x} - \frac{z_j F}{RT} D_j C_j \frac{\partial \phi(x)}{\partial x} + C_j v(x), \quad (5)$$

where $J_j(x)$ ($\text{mol cm}^{-2} \text{ s}^{-1}$) is a one-dimensional flux for species j at distance x (cm) from the electrode; D_j ($\text{cm}^2 \text{ s}^{-1}$), z_j , and C_j (mol cm^{-3}) are the diffusion coefficient, the charge, and the concentration for the species j ; $v(x)$ (cm s^{-1}) is the rate with which a volume element moves in solution; $\partial C_j(x)/\partial x$ is the concentration gradient and $\partial \phi(x)/\partial x$ is the potential gradient along the x -axis. In Equation (5), the first term is concerned with the diffusion and is actually Fick's first law, the second term accounts for the migration of the species in the solution, and the last term represents the convection of the solution. Pit or crevice propagation phase (above the pitting potential) is usually mass transfer controlled, e.g. Nernst–Planck equation is used. [5,33]

Another way to describe mass transfer is by Fick's law of diffusion. Fick proposed two laws of diffusion in a solution. These equations describe the relation between the flux of a substance and its concentration as a function of both time and position. The first law describes the flux

of a species O as a function of the change in its concentration C_O (mol cm⁻³) with distance x (cm) from an electrode, at a time t (s):

$$-J_O(x, t) = D_O \frac{\partial C_O(x, t)}{\partial x}, \quad (6)$$

where $J_O(x, t)$ (mol cm⁻² s⁻¹) is the flux of species O , and D_O (cm² s⁻¹) is the diffusion coefficient. The second law relates the change in concentration with time to the change in flux with position:

$$\frac{\partial C_O(x, t)}{\partial t} = D_O \left(\frac{\partial^2 C_O(x, t)}{\partial x^2} \right). \quad (7)$$

When the goal is to interpret data, the complexity of the mass transfer equations is usually reduced. This can be accomplished by minimizing the effects of convection, for example, by using stationary conditions (no stirring). Migration can be reduced by adding a supporting electrolyte to the solution to carry the current and to minimize the solution resistance and potential gradient. The appropriate supporting electrolyte should be inert and present in high concentration. [33]

3.2.2.3 Corrosion rate

When corrosion rate is to be determined, Faraday's law is a common option. A combination of Faraday's first and second law of electrolysis summarizes the equivalence between the amounts of chemical change and electrical energy involved in an electrochemical reaction. The rates of the anodic and cathodic reactions must be equivalent, as determined by the total flow of electrons from the anode to the cathode, known as the corrosion current, I_{corr} . Under freely corroding conditions the anodic and cathodic currents (not current densities) are equal (but opposite in polarity) and the corrosion potential attains a level at which equality occurs, i.e. both the anodic and cathodic reactions are polarized from their equilibrium values towards the corrosion potential. The corrosion rate (mpy) can be calculated from corrosion current using the Faraday's law:

$$CR = \frac{M_w I_{corr}}{ZFA\rho}, \quad (8)$$

where M_w is the molecular weight of metal (g/mol), I_{corr} is the corrosion current calculated from experiments (A), Z is the number of electrons transferred during electrochemical reaction, F is the Faraday constant (96,487 C mol⁻¹), A is the area of the working electrode (cm²) and ρ is the density of the metal (g/cm³). [14]

3.3 Experimental work on crevice corrosion

3.3.1 Alavi and Cottis experiment

Alavi and Cottis [34] conducted an experiment on crevice corrosion of stainless steel 304 (18% Cr, 8% Ni) and 7475 aluminium alloy (4.7% Zn, 2.1% Mg). The electrolyte used in both cases was 0.6 M NaCl solution of pH 6. The artificial crevice, the dimensions which were 8 cm in depth, 2.5 cm in length and 90 μ m in width, was formed between a plate of the metal being studied, embedded in epoxy resin, and a Perspex electrode holder. The steel was coupled to a larger piece of the same steel which was exposed to free-corrosion conditions in the aerated bulk electrolyte. The measuring electrodes were located in rows at 0.35, 1, 2, 4, and 7.5 cm from the crevice opening. Chemical reactions were assumed to occur in the system as listed in Table 4.

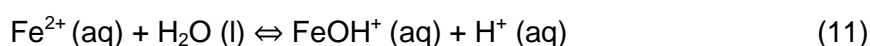
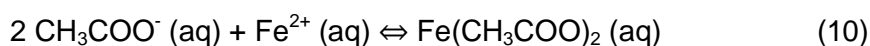
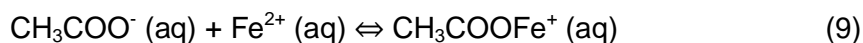
Table 4. Reactions assumed to occur in the system. [4]

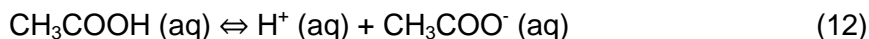
Reactions in the system	Reactions at metal/solution interface
1. $\text{Cr}^{3+}(\text{aq}) + \text{H}_2\text{O}(\text{l}) \rightleftharpoons \text{Cr}(\text{OH})^{2+}(\text{aq}) + \text{H}^+(\text{aq})$	1. $\text{Fe}(\text{s}) \rightleftharpoons \text{Fe}^{2+}(\text{aq}) + 2\text{e}^-$
2. $\text{Cr}^{3+}(\text{aq}) + 2 \text{H}_2\text{O}(\text{l}) \rightleftharpoons \text{Cr}(\text{OH})_2^{2+}(\text{aq}) + 2\text{H}^+(\text{aq})$	2. $\text{Cr}(\text{s}) \rightleftharpoons \text{Cr}^{3+}(\text{aq}) + 3\text{e}^-$
3. $\text{Cr}^{3+}(\text{aq}) + 3 \text{H}_2\text{O}(\text{l}) \rightleftharpoons \text{Cr}(\text{OH})_3(\text{aq}) + 3\text{H}^+(\text{aq})$	3. $\text{Ni}(\text{s}) \rightleftharpoons \text{Ni}^{2+}(\text{aq}) + 2\text{e}^-$
4. $\text{Cr}^{3+}(\text{aq}) + 4 \text{H}_2\text{O}(\text{l}) \rightleftharpoons \text{Cr}(\text{OH})_4^-(\text{aq}) + 4\text{H}^+(\text{aq})$	
5. $2\text{Cr}^{3+}(\text{aq}) + 2 \text{H}_2\text{O}(\text{l}) \rightleftharpoons \text{Cr}_2(\text{OH})_2^{4+}(\text{aq}) + 2\text{H}^+(\text{aq})$	
6. $3\text{Cr}^{3+}(\text{aq}) + 4 \text{H}_2\text{O}(\text{l}) \rightleftharpoons \text{Cr}_3(\text{OH})_4^{5+}(\text{aq}) + 4\text{H}^+(\text{aq})$	
7. $\text{Cr}^{3+}(\text{aq}) + \text{Cl}^-(\text{aq}) \rightleftharpoons \text{CrCl}^{2+}(\text{aq})$	
8. $\text{Cr}^{3+}(\text{aq}) + 2 \text{Cl}^-(\text{aq}) \rightleftharpoons \text{CrCl}_2^{2+}(\text{aq})$	
9. $\text{Fe}^{2+}(\text{aq}) + \text{Cl}^-(\text{aq}) \rightleftharpoons \text{FeCl}^+(\text{aq})$	
10. $\text{Fe}^{2+}(\text{aq}) + 2 \text{Cl}^-(\text{aq}) \rightleftharpoons \text{FeCl}_2(\text{aq})$	
11. $\text{Fe}^{2+}(\text{aq}) + 4 \text{Cl}^-(\text{aq}) \rightleftharpoons \text{FeCl}_4^{2-}(\text{aq})$	
12. $\text{Ni}^{2+}(\text{aq}) + \text{Cl}^-(\text{aq}) \rightleftharpoons \text{NiCl}^+(\text{aq})$	
13. $\text{H}_2\text{O}(\text{l}) \rightleftharpoons \text{H}^+(\text{aq}) + \text{OH}^-(\text{aq})$	

The variation of potential along the crevice with time and the corresponding pH changes were measured. The final pH values were in the range of 1.7 - 2.7. The most acidic values were obtained at 2 cm from the opening, whilst the least acidic values were found at the site farthest from the crevice mouth. Crevice pH and potential values for the crevices in type 304 stainless steel follow the classical pattern of crevice corrosion, with the crevice potential being more negative than the external potential, the crevice becoming acidified and corroding actively. There are indications that, in contrast to expectations, the chloride activity in the crevice in type 304 stainless steel does not increase during crevice corrosion. It is possible that this results from the rather wide crevice gap used in this work, or from complexation of the chloride leading to a reduced activity coefficient for chloride. [34]

3.3.2 Valdes-Mouldon experiment

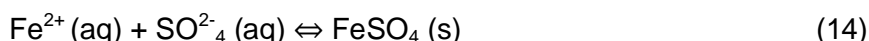
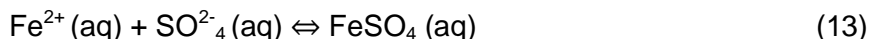
Valdes-Mouldon [34] conducted several experiments involving crevice corrosion of iron in electrolyte solutions. The experimental crevice was 10 mm deep, 5 mm wide, with a gap of 0.5 mm and iron metal on one side. A perpendicular section of iron, measuring 5 mm by 20 mm at the surface of the crevice, was anodically polarized to different potential values. The experiments were carried out with acetate buffer and sulfuric acid solutions. Valdes-Mouldon experiments considered systems having strong active/passive transitions and the associated potential changes were very high. The acetate buffer solution consisted of equal parts 0.5 M acetic acid and 0.5 M sodium acetate solution at 25°C. This formed a buffer solution with pH 4.8. The four principal reactions occurring in the system were considered:





These reactions involved seven aqueous species as well as water. Valdes-Mouldon conducted the experiment with the system anodically polarized to two different values. Valdes observed significant potential drops in the bulk solution outside the crevice mouth, and that the experimental crevices corroded most rapidly just inside the mouth.

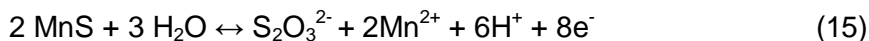
Valdes-Mouldon [35] also performed experiments in sulfuric acid electrolyte using the same machined crevice. The sulfuric acid solution was 0.001 M sulfuric acid at 25°C. The reactions involved were (five aqueous species + water):



The experiments made by Alavi and Cottis and Valdes-Mouldon are often used as validation results for different models. [4]

3.3.3 Thiosulphate entrapment experiment

Alkire et al. [36] developed and tested an idea of crevice corrosion initiation based on dissolution of MnS inclusions within the crevice. Anodically dissolving bulk samples of MnS in 0.1 M NaCl, it was shown that the electrochemical oxidation of MnS produced both thiosulphate ions ($\text{S}_2\text{O}_3^{2-}$) and protons, and that further dissolution of MnS also occurred to produce elemental sulphur (Equations 15 and 16). The experiment considered dissolution of evenly spaced inclusions together with passive dissolution of the steel 304 within the crevice. Dissolution of MnS produces elemental sulphur:



Later studies showed that when performing chemical analysis of solution extracted from crevices of 304L stainless steel during the induction period of crevice corrosion, the dominant sulphur species was sulphide (HS^-) instead of thiosulphate. This was also shown to be the main product of chemical MnS dissolution and the rate of such chemical dissolution was expected to be much greater than the electrochemical dissolution rate. Nevertheless, sulphide is equally capable of activating metal dissolution. The idea of Alkire et al. was tested by Laycock et al. [37] for 316 L stainless steel. They measured crevice corrosion initiation potentials and induction times for 316L stainless steel under open circuit conditions in 1 M NaCl with sodium hypochlorite added as an oxidant. They found out that crevice corrosion initiated at potentials much lower than the potentials where electrochemical dissolution of MnS was observed in sulphate solutions. Chemical dissolution of inclusions, possibly enhanced by partial acidification of the crevice, could lead to some thiosulphate accumulation, although not enough to cause general corrosion. Pitting could be enhanced within the crevice, but low (5 mM) levels of thiosulphate were shown to have little effect on the pitting potential of the 316L steel.

3.3.4 Pitting as a precursor of crevice corrosion

Based on the idea of pitting being a precursor of crevice corrosion and IRDT theory (Chapter 2.5.5 and 2.5.1), Shu et al. [24] conducted experiments to determine the induction period of crevice corrosion. In this experiment, commercially pure iron (ASTM A848) and 0.2 M Na_2SO_4 + 0.025 M K_2CrO_4 at pH 8.8 open to air were used to study of the induction period and transition to crevice corrosion. A rectangular crevice was used. The crevice's walls being vertical, and one wall of the crevice was of iron, with the other walls were transparent Plexiglas. The setup allows in-situ measurement of potential and solution composition

distribution as a function of time and distance x into the crevice, and real time visual and electronic monitoring of corrosion on the crevice wall. During the crevice experiments, the sample was anodically polarized to a passive potential of $E_{app} = 650 \text{ mV}_{SCE}$.

In-situ visual examination and ex-situ microscopy revealed that the first corrosive attack on the (passive) crevice wall generates as a pit near the bottom of the crevice (Fig. 14). Additional pits form progressively higher on the crevice wall through the induction period. The most favoured location on the sample for the cathodic reaction is within the pit which yields the smallest local cell circuit and therefore the smallest possible circuit resistance. The induction period ends as crevice corrosion begins at the location just above the last-to-form pits on the crevice wall. The fact that the prior pit growth processes were observed to cease in this transition and following crevice corrosion periods, further identifies the IR nature of the crevice corrosion since the active region now extends to the bottom of the crevice. IR theory is in this study used to explain the formation of pits on the crevice wall before conditions are set for the onset of crevice corrosion. The gas bubbles formed inside the pits and the changes in currents indicated that the pitting initially is a local cell process of metal dissolution and cathodic reactions on the sample. [24]

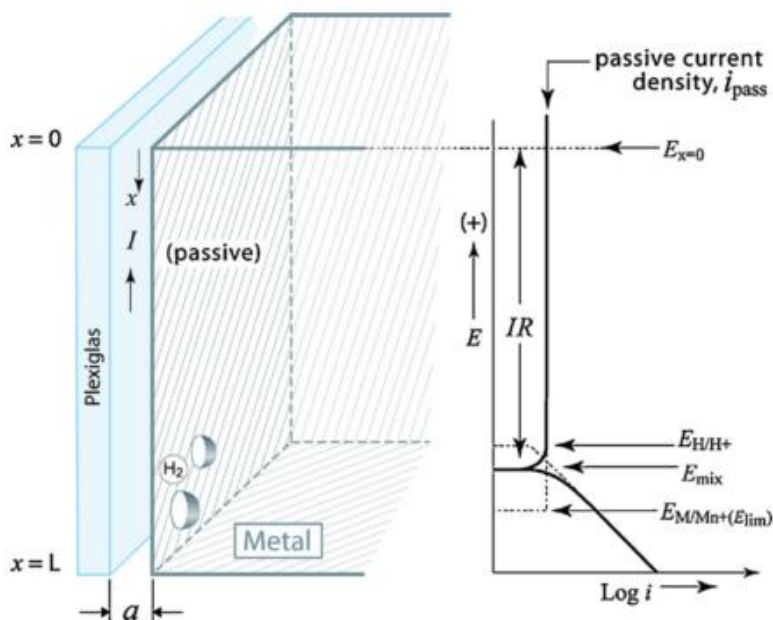


Figure 14. Schematic drawing showing pits initially forming at the bottom of the crevice wall during the induction period which precedes the start of crevice corrosion, and a passive polarization curve along the crevice wall for a crevice whose only opening to the bulk electrolyte is on the top surface. [24]

3.3.5 Passive dissolution experiment

Several studies based on passive dissolution e.g. CCS theory (Chapter 2.5.2) have been performed [1][37]. It was found that as a contradiction to CCS theory the change in crevice pH might be the result and not the cause of crevice corrosion. Laycock et al. [37] studied the initiation of crevice corrosion in stainless steels. The measurements of the potential and induction time indicated that the initiation of crevice corrosion on type 316L stainless steel in 1 M NaCl with sodium hypo-chloride added as an oxidant occurs after times an order of magnitude longer than the time taken for the peak metal ion concentration to be reached at the crevice center. At that time the pH in the crevice was not low enough to cause general corrosion. The CCS theory predicted also that crevice corrosion would initiate at the deepest point of a crevice where the most aggressive solution should be present as a result of mass transport processes, but this is not always observed in practice. [1]

3.3.6 Calculating coupling current

A study concerning coupled environment theory (Chapter 2.5.3) is demonstrated by Lee et al. [25] They developed a simple crevice corrosion monitor that employs the electron coupling current. Monitor was used to follow the development of crevice corrosion in mild steel 1018, type 304 SS and type 410 SS in deionized water and in sodium chloride solutions with and without corrosion inhibitor (anodamine). Tests were conducted by measuring the coupling current with GAMRY potentiostat which was used as ZRA. It appeared that the monitor detected crevice inversion and provided a convenient tool for determining inhibitor efficiency in reducing crevice activity in mild and stainless steels. Conclusions made from the experiments were: 1) monitor accurately follows the evolution of crevice activity in terms of the cathodic process that occurs on the external surface (oxygen reduction) and that develops within the crevice due to the accumulation of H^+ , 2) crevice initiation time is very short (less than 2 hours for tests reported here), but appears to depend upon the chloride concentration and possibly on the inhibitor concentration, 3) coupling current increases with time after initiation, passes through maximum and then decreases, eventually changing sign to mark the crevice inversion, and 4) in the absence of charge-compensating anion (in this case chloride), crevice corrosion does not initiate, as there is no means of balancing the positive charge being injected into the crevice by metal dissolution. [25]

3.4 Empirical crevice corrosion models

3.4.1 Empirical model for localized corrosion

In the study by Hakkarainen [38] an empirical model for predicting the possibility of localized corrosion in stainless steels was developed. The environmental factors considered in the model were temperature, pH, chloride content, sulphate content, presence of oxidizing agents, crevices, deposits, flow rate and possibility of concentration of solution by evaporation. The basic idea was to develop simple mathematical equations for the effects of all the factors to localized corrosion. According to the results of these equations, each factor will have suggestive values for the corrosion probability. For the first stage only chloride induced attack was considered at temperature ranges of 0 – 100 °C. The probability of an attack is estimated by comparing the “effective” chloride content of the environment to the “critical” chloride content values under service conditions. Temperature influences the “critical” chloride content: the lowest chloride content able to cause pitting attack of specific steel is lower at higher temperature. The ability of a continuous flow to diminish the possibility of pitting attack is also taken into account, as well as the increased corrosion possibility caused by crevices and deposits. According to the results it seems that trends reflecting the effects of the factors influencing localized corrosion can be written into equations and used as a predicting tool. [38]

3.5 Statistical crevice corrosion models

A statistical model was proposed by Williams et al. [39], where they modelled the pitting process as a series of events which were randomly distributed in time and space over the metal surface. Each event results in a local current which evolves with time according to rules which are the same for every event, and the total current is obtained as the sum of the local currents. Objective of the work was to take some steps towards a more rigorous definition of the parameters of a statistical model so that the potential and concentration dependences can be modelled. According to the model, pits are unstable when they are first nucleated, but if a pit survived past the critical age, it became stable. The model needs experimental data analysis to fit into a particular system, and it simplistically assumes that each micro pit had an equal chance of propagating into a macro pit, which disregards the role played by the microstructure, the local microenvironment and any aspect of the pit itself (for example the narrowness of the mouth or the existence of a pit cover). [5,39]

In a study by Laycock et al. [28] a deterministic model for the growth of single pits in stainless steel has been combined with a purely stochastic model of pit nucleation. Monte-Carlo methods have been used to simulate experiments on samples with a large number of possible pitting sites, and the results are compared against experimental data from both potentiostatic and potentiodynamic experiments. Anodic and cathodic reactions in the concentrated pit solutions are modeled on a semi-empirical basis, with parameters for a particular set of conditions determined by comparing the predictions of the model against experimental results from various artificial pit experiments. In this model also surface roughness is taken into account by considering pit initiations to occur within cone-shaped depressions of depth d . By increasing the value of d therefore corresponds to increasing surface roughness, and d distributions approximately match to the R_a values produced by common grit finishes. The pitting potentials obtained in model simulations are determined mainly by the pit propagation element, and a limiting lower bound distribution of the pitting potential can be calculated without any consideration of pit nucleation processes. The quantitative agreement between model and experiment is reasonable for both 304 and 316 stainless steel, and the effects of varying surface roughness, solution chloride concentration and potential sweep rate have been considered.

3.6 Mechanistic crevice corrosion models

3.6.1 Point defect model (PDM)

The most atomistically based model available for the prediction of localized corrosion sensitivity is the point defect model (PDM) [40]. The PDM considers the transport of cation vacancies in the passive film towards the film–metal interface, where they can condense to form voids or developing pits at the metal–passive film interface if the flux of vacancies arriving at the interface is greater than what can be consumed by annihilation via a metal oxidation reaction. The effect of an aggressive species, such as Cl^- , is hypothesized to alter the generation and transport of cation vacancies. The model correctly predicts the logarithmic dependency of pit initiation potential on Cl^- concentration, the effects of some alloying elements, and the effect of parameters such as scan rate on pit initiation. In a recent development of the PDM, Macdonald et al. modelled the inhibitive effect of oxyanions, such as NO_3^- and BO_3^- , on pit breakdown potential of 316L stainless steel by considering the competitive adsorption of aggressive and inhibitive species at O vacancies at the film–solution interface. The model predicts that the breakdown potential should vary with:

$$\log \left(\frac{[X^-]}{[Y^z-]} \right), \quad (17)$$

where $[X^-]$ is the concentration of aggressive species such as Cl^- and $[Y^z-]$ is the concentration of inhibiting oxyanions. Experimental results found this relationship to be true for 316L stainless steel in $\text{Cl}^- + \text{NO}_3^-$ -solutions.

Assumptions made in PDM are [40]:

- The electric field strength is constrained to an upper limit of about 5 MV/cm by electron-hole pair generation via Esaki tunnelling (Esaki diode is a p-n junction device that exhibits negative resistance; when voltage is increased the current through it decreases)
- The electric field strength is independent of the applied voltage, implying the rate control resides at the metal/barrier layer interface
- The barrier layer dissolves at the barrier layer/solution (outer layer) interface by either chemical or electrochemical processes

- Potential differences exist across the metal/barrier layer and the barrier layer/outer layer (solution) interfaces
- Potential difference across the barrier layer/solution (outer layer) interface is a linear function of the applied voltage and pH

Disadvantages of the PDM focus on the linearization of the transport equations and on the handling of the potential drop at the oxide/electrolyte interface. The PDM predicts the pitting potential, whereas the breakdown occurs at much lower potentials. A bilogarithmic dependence of pitting potential on Cl^- concentration is often observed, but is not predicted by the PDM at present. The PDM does not explain why breakdown is localized at discrete sites. [5,7]

3.6.2 Coupled environment models

A mathematical model for estimating concentration and potential distributions inside and outside crevices with porous walls that are permeable to oxygen and open to a thin electrolyte film on the external surface has been developed. A study by Engelhardt et al. [16] investigated a model where corrosion of steels takes place in a thin, narrow crevice formed between the metal surface and an oxygen-permeable, porous deposit. On the deposit, a thin electrolyte layer exists, due to geochemical fluids dripping onto a deposit-covered surface or adsorption of moisture, when hygroscopic deposit is considered. In Fig. 15, an example of the studied crevice geometry is presented. The model is based on the determination of the system mass transfer equations along with the equation of electroneutrality. The main mass transfer equations were kept in rate format, i.e. chemical terms were used in normal form without eliminating the chemical terms by adding and subtracting the mass balance equations, which allows generalization of the computer code to the case of a random number of chemical and electrochemical reactions. Mass transfer by diffusion and ion migration is considered in both the electrolyte films inside and outside of the crevice. The main chemical reactions considered are the anodic dissolution of the alloy substrate, hydrolysis of the alloying element cations (Reaction 11 in Table 3), dissociation of water (Reaction 13 in Table 3), and the cathodic reduction of oxygen, hydrogen ion, and water (Reactions 2 and 3 in Table 3). In the study seven species were considered (Me^{2+} , $\text{M}(\text{OH})^+$, Na^+ , Cl^- , H^+ , OH^- , and O_2), where, for simplicity, alloy dissolution can be simulated by the dissolution of a metal, Me. The effect of parameters connected with the porous layer (porosity, tortuosity, and the layer thickness) has been taken into account by using a mass permeability coefficient K when considering the rate of crevice corrosion. K can be presented in the form:

$$K = \frac{\varepsilon D_7}{\tau^2 h}, \quad (18)$$

where ε is the porosity, τ is the tortuosity, D_7 is the diffusion coefficient, and h is the width of the wet part of the porous deposit. A special relaxation procedure had been used to ensure the integration of the solution in the presence of very fast chemical reactions. All thermodynamic and kinetic data needed for this study (the corrosion data of carbon steel in chloride solutions, and kinetic parameters for oxygen reduction) was taken from available studies. [16]

In the study by Engelhardt et al. [16] it was shown that the crevice acts as an 'electrochemical amplifier' when investigating the concentration of aggressive anions that leads to an increase in the corrosion rate and to a higher probability of pit nucleation within the crevice. Calculations performed in this study show that the effect of a porous layer increases with decreasing mass permeability K . For some particular series of parameters, the critical values of the permeability coefficient for inactivation of the crevice, K_{cr} , has been estimated. When $K < K_{cr}$, some critical conditions can be distinguished and the crevice corrosion can be initiated. It has been shown that the influence of the porous layer is lowered by decreasing the passive corrosion current density and increasing the width of the crevice.

In addition, describing the conditions that exist within a corroding crevice with permeable and non-permeable walls, and which opens to a thin electrolyte film on the external surface, it is impossible to neglect the concentration and potential drops in the external environment (outside the crevice). The concentrations of the main components that define the conductivity of electrolytes (Me^{2+} , Na^+ and Cl^-), and therefore the conductivity of the film, can differ significantly outside the crevice. This means that prediction of the potential distribution along a metal surface covered with a thin electrolyte films must be done generally by solving the full system of mass transfer equations together with the local electroneutrality condition (Chapter 2.5.3 Coupled environment theory). In conventional modelling of crevice corrosion the models calculate the potential distribution by solving the balance equations only for the environment inside the crevice, which can lead in some cases to significant error. [16]

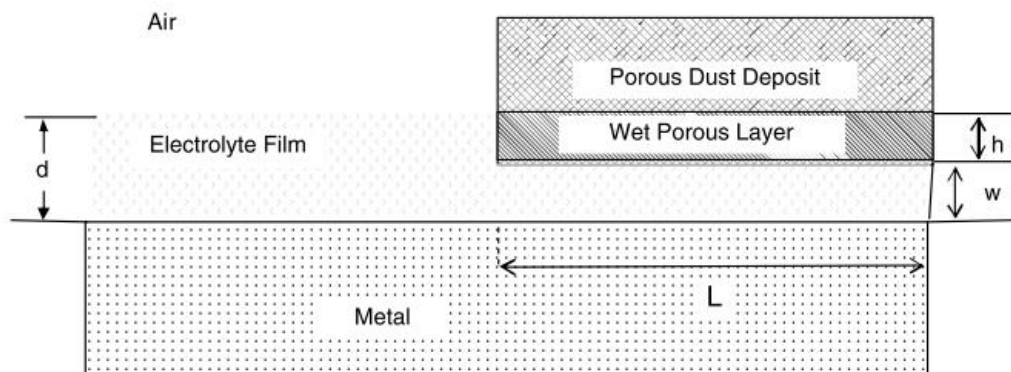


Figure 15. Geometry for crevice corrosion under an oxygen-permeable deposit. [16]

3.6.3 Critical crevice depth method

One important task in describing crevice corrosion is to develop a way to predict which geometries will be sensitive to crevice corrosion and to determine the critical crevice geometry that separates the region where crevice corrosion initiates from that where crevice corrosion does not occur. In cases, when the crevice corrosion cannot be avoided, the prediction of the corresponding corrosion damage as a function of time is essential. In this study Engelhardt and MacDonald [41] estimated the magnitude of crevice corrosion damage, which is expressed as the maximum penetration into the crevice wall. It has been suggested that different mechanisms should be used to describe the initiation of crevice corrosion in different geometries. Usually the initiation of crevice corrosion is connected to the development of a differential aeration cell with the following acidification of the crevice solution and/or migration of aggressive anions (for example, Cl^-) into the crevice. However, this is not able to explain cases of instant corrosion or cases of crevice corrosion in systems which show no significant acidification or aggressive ion build-up in the crevice solution. In these cases, crevice corrosion can be caused by IR potential drop in the crevice, which places the local metal potential existing in the crevice wall in the active dissolution region of the polarization curve. Generally, if no significant concentration drops in the crevice appear, the IR drop can be calculated by solving a Poisson-type differential equation relative to the potential in the solution by using a numerical method. The Poisson-type equation is defined as:

$$\frac{d^2 E}{dx^2} = \frac{i_s(E)}{\kappa w} \quad (19)$$

where κ is the conductivity of the electrolyte, w is width of the crevice, E is the potential of the metal, i_s is the charge transfer current density entering the crevice at the metal crevice wall, and x is the distance from the crevice mouth into the crevice. Such calculations lead to the definition of the location of the active–passive transition and to the definition of the critical crevice depth L_c . The critical crevice depth is defined as the depth, which is measured from

the crevice mouth, at which the active–passive transition just occurs within the crevice. Study also shows that the crevice can remain passive, even when its depth is greater than the critical value. [41]

The study by Engelhardt and Macdonald [41] considers the case when the potential distribution inside a corrosion crevice obeys Ohm's law. It was shown that the potential and current distributions in the crevice depend not only on the metal potential, conductivity of the solution, and on the geometry of the crevice, but also on the history of crevice corrosion initiation. Generally, the conditions in the crevice (active or passive dissolution) will depend on any process that leads to the localized or general depassivation of the crevice walls. It is suggested that a simple relation could be used for estimating the L_c as a function of w , κ , E , and a polarization curve. It was also shown that L_c is proportional to $\sqrt{w\kappa}$ and is the linear function of E . Calculation of the corrosion damage (maximum depth of the penetration into the metal, w_{max}) as a function of time and position inside the crevice has been performed for different values of E . Calculation of the corrosion damage (metal loss) as a function of time and position inside the crevice has been performed for different possible potential distributions, and it is found that the calculated damage agrees very well with the experimentally measured damage. It was shown that, during the initial stages of crevice corrosion, when the one-dimensional approximation is valid, w_{max} is determined mainly by the polarization curve for the anodic dissolution of the metal. It is also shown that, in general, it is impossible to neglect the potential drop in the external environment when quantitatively describing crevice corrosion. [41]

3.6.4 Combined IR drop theory and CCS model

A mathematical model combining the theories behind IRDT and CCS model was suggested by Kennell et al. [18] The model couples anodic areas within the crevice with cathodic areas on the bold surface, e.g. the same idea as in Coupled environment theory (Chapter 2.5.3). It also incorporates the combined effects of the chemical attack of the crevice solution along with the electric potential changes in the crevice and over the bold surface (accounts for the potential drops between these areas). The model is used to predict the dynamic crevice pH profile according to the experimental data of Alavi and Cottis [34] by using a one dimensional computational grid (Fig. 16). The mass transport approach considered in this model takes diffusion, electromigration, diffusion potential, charge density constraints, and a source or sink of chemical species due to chemical reactions into account. Also electroneutrality is considered. For chemical reactions kinetic behaviour is neglected. The electrode kinetics concerning cathodic and anodic currents are solved separately, and then balanced in the model by finding the potential at the interface (the crevice mouth) between the two that causes equal cathodic and anodic currents.

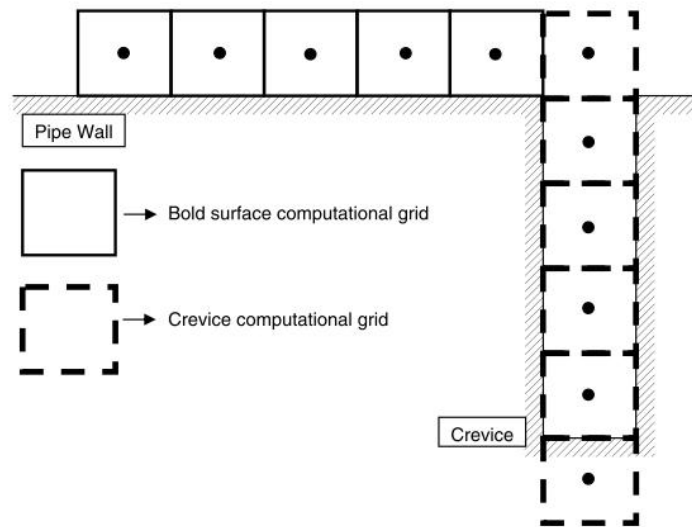


Figure 16. Computational grid used in the model.[18]

Three new phases of crevice corrosion were theorized in the study: the total corrosion phase, the dynamic phase, and the quasi steady-state phase. These three phases show how the corrosion in the crevice changes from a uniform passive current to an active corroding region near the crevice mouth with an extinct region near the crevice tip. Fig. 17 shows the validation of the current model against the experimental data of Alavi and Cottis and five of the leading published crevice corrosion models that were also used to simulate the same experimental data. It can be seen that the combined IRDT and CCS model describes quite well the real behaviour compared to the other models. The model predicts correctly the shape of the pH profile along the length of the crevice. It predicts that pH at the tip is higher than the pH at the mouth, and that the minimum of pH is located about 1 cm from the crevice mouth, which fits well to the experimental data. [18]

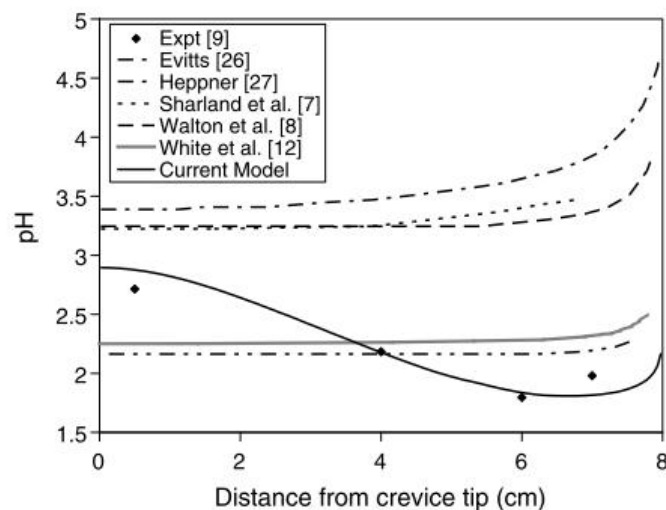


Figure 17. Comparison of published models and experimental data for a corroding AISI 304 stainless steel crevice. [18]

3.6.5 Computational model for incubation of crevice corrosion

Heppner et al. [31] created a generic mathematical model to predict the crevice corrosion incubation period, i.e., time from immersion to active crevice corrosion, of four passive metals and alloys. The model could be used in the selection of alloys for corrosive operation environments. The computer model calculates crevice solution composition as a function of

space and time. The model has little empirical limitations making it suitable for extrapolation. The key factor in the successful modelling of crevice corrosion is correctly determined electrochemical dissolution at the metal-solution interface. The model assumes that the passive current controls the passive corrosion rate. The passive current depends upon the average valence charge of the metal dissolution products, which determines the passive currents response to changes in pH. The level of the passive current also depends on the magnitude of the activation energy, which determines the passive currents response to thermal effects. The crevice solution composition at steady state is highly dependent upon the magnitude of the passive current. The model has an algorithm developed to adjust crevice solution composition for chemical and electrochemical equilibrium (rapid approach of chemical equilibrium is assumed). Equilibrium expressions are assembled at run-time from a generic equilibrium description. The model utilises infinite dilution theory and is capable of reaching a steady state. The transport model used in this work considers transport caused by diffusion, electromigration, diffusion potential, charge density, chemical reaction, and electrochemical reaction. One-dimensional finite difference grid is used in discretization of transport problem. Based on theoretical principles, the Poisson Equation is solved to bring the system near electrically neutral conditions. The Poisson term is:

$$\frac{z_i u_i F^2 C_i}{\epsilon} \sum_j z_j C_j, \quad (20)$$

where ϵ is permittivity (Farad/m), u is mobility ($\text{m}^2\text{mol}/\text{Js}$), z_i is charge number of species i , F is Faraday constant, C is molar concentration (mol/m^3). Equilibrium constants and transport properties are adjusted also for elevated temperature. The corrosion rate is modified for thermal and acidity effects via an Arrhenius expression and a Freundlich isotherm. The Freundlich adsorption equation is:

$$\log i_p = \log k - npH, \quad (21)$$

where n is the number of reactions, i is passive current density (A/m^2), and k is equilibrium constant. No assumptions are made upon the nature of the metal or alloy in the implementation of this model. The lack of assumptions in this algorithm allows for any complete set of chemical and electrochemical reactions to be solved.

The incubation periods of four industrially important metals (304 stainless steel, 316 stainless steel, Hastelloy C-276, and titanium) have been modelled at 298 K and ranked. Results indicated that: 1) titanium had an infinite incubation period, 2) Hastelloy C-276 had an infinite incubation period (more closely approaches the critical crevice solution pH as compared to titanium), 3) Type 316 stainless steel had an incubation period of approximately 30 min, and 4) Type 304 stainless steel had an incubation period of approximately 5 min. Predictions are in line with crevice corrosion theory and match experimental observations. All information is read from specially formatted text files at run-time adding flexibility to the model. The user may design these text files using an application developed as a complement to the computer model. However as with any simulation package, the quality of simulation results is highly dependent upon quality of parameters supplied by the user. [8,31]

3.6.6 FEM model of the propagation of crevice corrosion and pits

The model used in a study by Sharland et al. [27] considers the time evolution of the solution chemistry and electrochemistry within an active crevice, and uses the method of finite elements to solve the complex set of mass-conservation equations describing the system. It is applied to pitting and crevice corrosion in carbon steel and is demonstrated by testing various predictions against experimental data. Aim of the work by Sharland et al. [27] is to develop a mechanistic model of the propagation of an established pit or crevice, based on a mathematical representation of the physical mechanisms controlling the process, which will eventually be used as a predictive tool. The model presented in this work involves dividing the crevice into a series of finite elements and solving the equations governing the chemistry

and electrochemistry in the crevice using this grid. The model uses the CAMLE computer program based on HARWELL finite-element subroutine. This approach allows a more complex description of the solution chemistry in the crevice, and may be applied over a wider range of physical and chemical conditions. This technique also allows a time-dependent description of crevice corrosion propagation. In the model, the pit or crevice is assumed a parallel-sided slot, filled with a dilute solution of sodium chloride (Fig. 18). A typical grid for a crevice with passive walls is illustrated in Fig. 19. The following assumptions are made:

- The metal surface outside the crevice is covered with a passive film and there is sufficient generation of cathodic charge on the outer surface to drive the localized corrosion
- The important effects are genuinely local; any changes or local variations in the chemical and electrochemical conditions within the crevice do not affect the potential of the whole specimen
- Transport in the through-thickness (z direction in Fig. 18) may be neglected, i.e. only variations along the depth and across the width of the crack need be considered, and the equations may be reduced to two dimensions or, for a crevice with passive walls, to one dimension
- The electrolyte is static and no fluid flow effects need to be included
- Crevice propagation is slow compared with the ionic migration rates, and both moving-boundary effects and any induced electrolyte motion may be ignored
- The crevice is anaerobic
- Dilute solution theory may be used throughout, and so the activity of water is not considered specifically.

The dilute-solution theory, the transport of aqueous species i by diffusion under concentration gradients, by electromigration under potential gradients and chemical reaction are considered in the modelling. Experimental data produced by Beavers and Thompson [42] was used in the modelling. The model seems quite successful at predicting certain measured quantities in the system, despite the simplifications made in the chemical description of the pit environment. In particular, the active-wall model agrees that the largest metal dissolution rates will occur at the pit mouth, suggesting that a real pit in carbon steel will tend to spread out as well as grow downward. If there are no significant cathodic reactions occurring within a pit, the model predicts that the downward propagation rate in a pit with active walls is about a factor of four less than that of a pit with passive walls (for this particular pit size and metal potential). For higher values of the metal potential or for narrower pits, this ratio will be higher. [27]

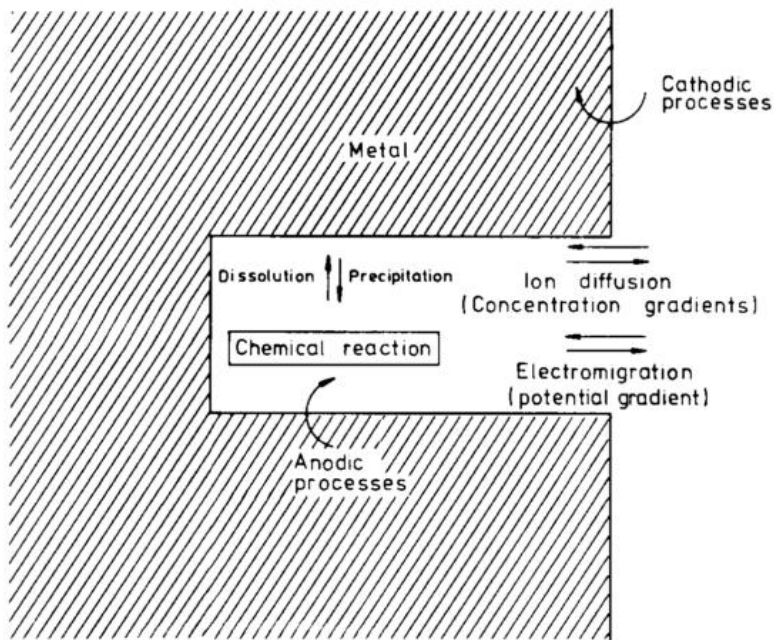


Figure 18. Schematic illustration of the processes included in the crevice corrosion propagation model. [27]

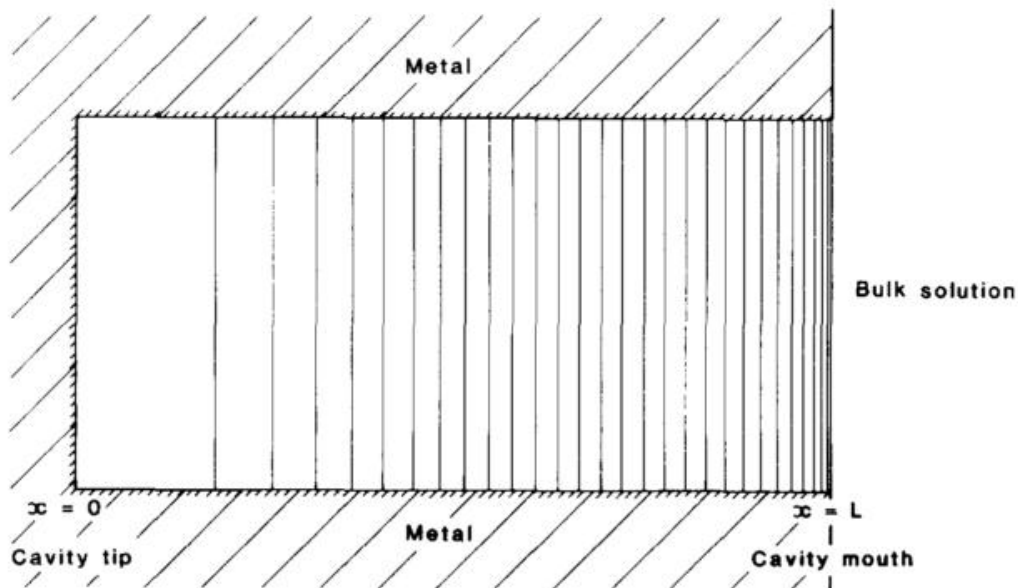


Figure 19. Finite-element grid used to solve mass-conservation equations in the model. [27]

An update to Sharland's model was proposed by Walton et al. [4] The goal of their work was to develop a crevice corrosion model that would be sufficiently general to be useful in a variety of applications. The model is capable of simulating processes such as crevice corrosion initiation, propagation rate of crevices (i.e. spatially dependent corrosion rate), and crevice repassivation as a function of external electrolyte composition and potential. The model can also simulate pitting corrosion growth. The model is applied to three experimental data sets including crevice corrosion initiation on stainless steel and active corrosion of iron in several electrolytes. In the corrosion area, the model utilises new ideas in three areas: 1) equations for moderately concentrated solutions including individual ion activity coefficients and transport by chemical potential gradients are used rather than equations for dilute solutions; 2) the model is capable of handling passive corrosion, active corrosion, and active/passive transitions in a transient system; 3) the code is general in format, including

evaluation of the importance of different species, chemical reactions, metals, and types of kinetics at the metal/solution interface.

The simulation domain in this model is broken into a set of calculational nodes (Fig. 20). Nodes can be non-uniformly spaced to increase accuracy where gradients are highest. The system of equations is solved by relaxation (weighted averaging of old and new values at each node) until convergence is obtained. The model considers unidirectional mass transport by diffusion and electromigration, and the electroneutrality is assumed. The experimental data by Alavi and Cottis [34] (NaCl solution), Valdes-Mouldon [35] (acetate and sulphuric acid system) was used in the modelling. The comparison of experimental and modelled data shows that the agreement between the results differs from approximate (Alavi and Cottis data) to very good (Valdes-Mouldon data). The imprecise predictions of Alavi and Cottis data are probably associated with changes in the passive current density with time during the course of the experiment (Alavi and Cottis data does not contain electrochemical kinetic data required by the model). The Valdes-Mouldon data was used to test the importance of activity coefficient treatment on modelling results. It was discovered that for the system modelled, the activity coefficients are relatively unimportant. Instead, full description of chemical reactions in solution (complex formation and hydrolysis) and the electrochemical reactions at the metal/solution interface are the most important factors required to accurately describe the chemical environment inside the crevice and the potential distribution. [4]

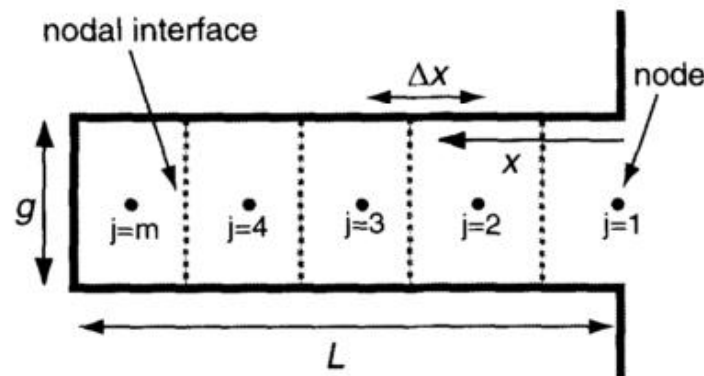


Figure 20. Schematic of model geometry for a crevice. Ion fluxes and current are calculated at nodal interfaces; concentrations and potential are calculated at node locations. g and Δx may vary with x . [4]

3.6.7 ALE (arbitrary Lagrangian–Eulerian) model

One of the challenges in the simulation of crevice corrosion propagation is the appropriate treatment of non-aqueous species (gas or solid), since the appearance of a new phase in a crevice will automatically have an impact on crevice's geometry. To overcome this challenge, moving mesh method could be a promising approach. An arbitrary Lagrangian–Eulerian (ALE) method is one of the moving mesh techniques, which includes advantages of the traditional Lagrangian-based and Eulerian-based finite element simulations. The ALE model is used in the study by Sun et al. [17] to predict the time-dependent evolution of the crevice geometry, the potential distribution, and the mass balance of a corroding crevice.

The experimental data by Alavi and Cottis [34] is used in the modelling. In the transient potential calculations, Ohm's law (Equation 22), the continuity equation (Equation 23) and Gauss law (Equation 24) are adopted to analyse the electrodynamics of the crevice corrosion system:

$$J = \sigma E \quad (22)$$

$$\frac{\partial \rho}{\partial t} + \nabla J = 0 \quad (23)$$

$$\nabla \cdot (\varepsilon E) = \rho, \quad (24)$$

where E is electric field strength (V/m), J is current density vector (A/m^2), σ is electric conductivity (S/m), ρ is charge density (C/m^3), and ε is relative permittivity. In the mass balance calculation, the conventional Nernst–Planck equation is applied to the mass conservation by considering diffusion, electromigration, electrolyte electroneutrality, hydrolysis reactions and electrochemical reactions. The electrochemical reactions that involved in the crevice corrosion process of AISI 304 stainless steel are described by Butler–Volmer and Tafel equations. Multistage hydrolysis reactions of the metallic ions and their complex reactions with anions, as well as the hydrolysis equilibrium of water, are taken into consideration. The crevice deformation velocity caused by the metal dissolution is presented by Faraday’s law, while the deformation by corrosion product deposition is obtained on the basis of the kinetics of corrosion product deposition. An example of the model concept is shown in Fig. 21.

The computations involving the partial differential equations of the model are performed by using the COMSOL Multiphysics software program, which allows flexible meshing of model geometry and setting of boundary conditions. The numerical results are in good agreement with the experimental results: the model reasonably well predicted the dynamic pH distribution inside the crevice. The model is also capable of predicting the corroded crevice shape and indicating that the deposition of corrosion product accelerates crevice corrosion. However, no experimental data for the kinetic rate of corrosion product deposition is available, which makes the prediction only qualitative. [17]

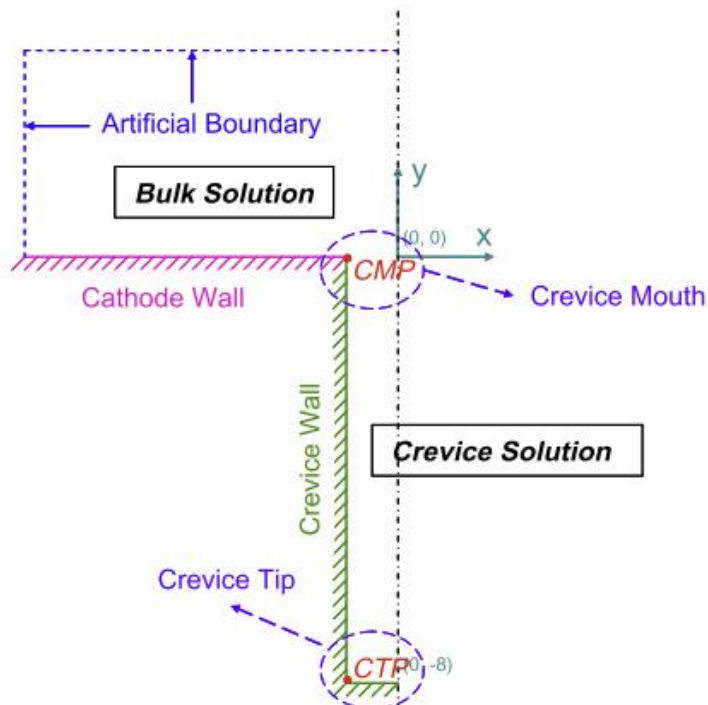


Figure 21. A schematic diagram of the crevice geometry and the concepts used in this work. CMP means crevice mouth position, and it is a reference position. CTP means crevice tip position. [17]

3.6.8 Cathodic focusing (CF) model

Cathodic reactions such as reduction of hydrogen (Reaction 3 in Table 3) and oxygen (Reaction 2 in Table 3) generate a single hydroxyl per electron consumed, and this chemical production has an alkalinizing effect. This process can make some areas of the crevice alkaline if significant amounts of the required cathodic current to support the dissolution reactions are found locally. At open circuit, the metal is no longer coupled to the outside surface of crevice and all of the required current is available locally. This alkalinizing effect can lead to the localization of attack near the crevice mouth. This model has been named the Cathodic Focusing (CF) model by Stewart [23]. The CF model differs from the standard crevice models in the literature so that it accounts for the effects of cathodic reactions occurring deep within crevices. The CF model, by its explanation of the retarding force against crevice corrosion, presents the possibility of strengthening that retarding force and stopping crevice corrosion entirely. In this study CF model is used to predict the intermediate attack of the crevice. Intermediate attack describes the commonly observed condition in crevice corrosion where the area nearest the crevice mouth is uncorroded, the next deepest area is heavily attacked, and the deepest regions are paradoxically unaffected by the corrosion. The functionality of CF model was tested using a CREVICER programme as a platform to model crevice corrosion under different sets of assumptions. CREVICER is a two-dimensional FEM code for the solution of time-varying partial differential equations used in modelling the chemical concentration and potential fields of crevices. It is capable of accounting for or disregarding any variables as needed.

Factors considered in the CREVICER modelling are diffusion, migration, charge neutrality, dilute solution, two-dimensional geometry, electrical and chemical flux, and temperature. Factors that were not considered were single ion activity, viscosity, pressure, convection, precipitation, and diffusion potential. The potential field is based on the Ohm's law. The diffusivity for each species used in CREVICER is calculated from the Nernst-Einstein equation. The Nernst-Einstein equation relates the diffusivity to the mobility, the gas constant and the temperature:

$$D_i = u_i RT, \quad (25)$$

where D_i is the diffusivity of species i (m^2/s), and u_i is mobility constant for species i ($\text{m}^2\text{-mol}/\text{J-s}$). The conditions of charge neutrality and chemical equilibrium are enforced after the transport of all the species for each time period. The functionality of CF model was tested for different cases, in which different simplifications and assumptions were made. The results showed that the CF model can describe intermediate corrosion attack, and that the CF model fully accounts for the electrical and chemical processes occurring inside crevices. However lots of extensive experimental work is required to prove the functionality of the model. [21,23]

3.6.9 Repassivation potential model

A mathematical model concerning repassivation potential (Chapter 2.5.4) was developed by Anderko et al. [22] The repassivation potential model considers the electrochemistry of a metal M that undergoes dissolution underneath a layer of concentrated metal halide solution MX . The system is regarded as one-dimensional, irreversible thermodynamic model combined with a model of thermodynamic speciation. Gibbs energy and enthalpy of activation are main parameters for determining repassivation potential. The model assumes that, at a given instant, the oxide layer covers a certain fraction of the metal surface. The model includes the effects of multiple aggressive and non-aggressive or inhibitive species, which are taken into account through a competitive adsorption scheme. Equation used in the calculation of E_{rp} is:

$$1 + \sum_i \left[\left(\frac{i_{rp}}{i_p} - 1 \right) \frac{l_i^n}{i_{rp}} \right] \theta_j^{n_j} \exp \left(\frac{\xi_i F E_{rp}}{RT} \right) = \sum_j \frac{k_j^n}{i_{rp}} \theta_j^{n_j} \exp \left(\frac{\alpha_j F E_{rp}}{RT} \right), \quad (26)$$

where, i_p is the passive current density, T is the temperature, R is the gas constant, and F is the Faraday constant. k_j^n is the rate constant for the reaction mediated by the adsorption of aggressive species j , k_i^n is the rate constant for the reaction mediated by the adsorption of an inhibitive species i , n_j is the reaction order with respect to species j , α_j and ξ_i are the transfer coefficients of the aggressive and inhibitive species, and θ is the partial coverage fraction of species j .

In the experimental part, laboratory and field measurements of E_{rp} and E_{corr} were conducted in a nearly saturated chloride brine using three MAS probes, each consisting of eight identical wires of stainless steel 316L (UNS S31603), AL6XN (UNS N08367) and alloy C-276 (UNS N10276). Nominal operating conditions involved a temperature of 100 °C, pH ranging from 8-10, and a superficial liquid velocity of 0.61 m/s through the loop. The primary corrosive component in the process brine is the chloride ion. The localized corrosion sensitivities of the three alloys were in agreement with the model predictions based on a comparison of the repassivation and corrosion potentials (Fig. 22). As a further step of model validation, the predicted localized corrosion rates were compared to the measured pitting rates in the process stream. [7,22]

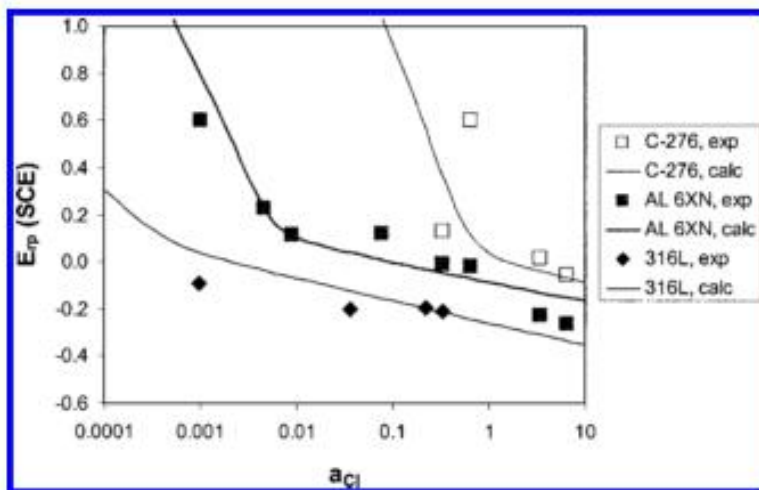


Figure 22. Calculated and experimental repassivation potentials for type 316L stainless steel and alloys AL6XN and C-276 at 60 °C. [22]

4 Discussion and conclusions

According to the studies made on crevice corrosion it seems that the most common reactions and equations (Chapter 3.2) are a good starting point for the modelling, though they have certain limitations and assumptions. Naturally the reactions and equations have to be modified to suit the inspected metal-environment combination, as has been done in most of the reviews. For mass transfer reactions in most models migration and diffusion are considered. When considering solution chemistry, it may be convenient to use the dilute solution theory for the modelling, although this is not recommended for real solutions. Activity coefficients that account for the non-ideal behaviour of charged species at non-dilute concentrations should be used where possible. What should be yet studied is the role of a passive film in the initiation of pitting corrosion, and the effect of self-repair process and electronic properties of the film. Another unknown factor is what happens in a pit or crevice during a very long pit initiation time (e.g. months, years). From the crevice corrosion models the ones that apply the coupled environment approach (Chapter 2.5.3) seem to have potential background for the modelling system, since they take into account the interaction between crevice and the external surfaces. The CCS theory alone is not able to explain the crevice corrosion initiation, as was mentioned by several authors [1]. The PDM is the most

atomistically based model for the prediction of localized corrosion sensitivity, and could therefore provide a very realistic base for the modelling [40]. The CF model has also potential by acknowledging the cathodic current inside the crevice, though the significance of this current to the overall current behavior needs more studying. Statistical models [28] show potential, since they take the partly random nature of crevice corrosion into account. [1,5,10,23,29]

Many models utilise FEM as a part of the modelling procedure, the quality of which depends greatly on the definition of the mesh and the boundary conditions. Formulation challenges arise in FEM when two or more apparently dissimilar modelling philosophies operating at different scales are combined to explain a phenomenon such as corrosion. Also the equations, which include terms that can lead to rapid variation in the solution, create challenges for FEM. As mentioned in Chapter 3.1 also meshless methods for modelling exist, that can have potential to handle the moving discontinuities. [5]

As the models develop more potential compared to the older models arise. For example the idea of using COMSOL as a modelling platform; the work load is greatly reduced since the basic structure (equations and reactions) is already in the package. When considering the amount of work that was needed to create the CREVICER model by Stewart et al. [23], it would reduce the amount of work as a new model base would not need to be built from scratch. The functionality of the interaction between the inserted equations and values in CREVICER in a long run after adding many new factors remains unclear. However, this is a common problem when ready-made platforms are being utilized.

The modelling of crevice corrosion has yet great challenges to overcome, since the processes taking part in crevice corrosion are not fully understood. Perhaps the most critical subjects to be solved are the real factors controlling crevice corrosion initiation, and determining the rates of attack in the crevice and the resulting changes in crevice shape. The distinction which of the observed changes in crevice conditions are results and which are the causes of crevice corrosion is important. [23]

As the approaches for crevice corrosion modelling consist of many different model configurations and try-outs, the best solution is rather difficult to distinguish. As a conclusion in Table 5 the reviewed empirical, statistical and mechanistic models are presented. The limitations and requirements of current models create great challenges for the modelling development. When considering the work load needed for corrosion modelling the use of ready-made multiphysics modelling platforms seems attractive. A modelling tool-box, that includes the needed databank (equations and reactions) and allows the needed modifications for different systems to be done, would reduce remarkably the modelling work effort. If it would be possible to add atomistic and molecular modelling to the model, the specific interactions between atoms and molecules could also be examined. Also a statistical tool should be incorporated to the model. The one perhaps most important requirement for ready-made modelling platforms is flexibility, since the platform needs to meet the challenge of ever developing knowledge of crevice corrosion.

Table 5. Summary of the studied models and their properties.

Model	Input	Theory/idea	Output
<i>Empirical models</i>			
Hakkarainen [38]	Own experiments	Simple mathematical equations for the critical Cl^- concentration for pit initiation	The probability of an attack is estimated by the effective chloride content
<i>Statistical models</i>			
Williams et al.[39]	Mathematical equations	Pitting is a series of events which were randomly distributed in time and space	Potential and concentration distributions
Laycock et al. [28]	Potentiostatic and potentiodynamic experiments	Deterministic model for the growth of single pits combined with a purely stochastic model of pit nucleation (Monte Carlo)	Pitting potentials
<i>Mechanistic models</i>			
PDM [7,40]	Concentration of aggressive species and inhibiting anions	Breakdown of passive film varies with concentration of aggressive species and inhibiting anions	Dependency of pit initiation potential on Cl^- concentration
Sharland et al. [27]	Experimental data by Beavers and Thompson	Dividing the crevice into a series of finite elements (FEM)	Rate of enlargement of pits or crevices as a function of metal potential, external solution chemistry and crevice dimensions
Heppner et al. [8]	Experimental data of Alavi and Cottis	Computer algorithm adjusts crevice solution composition for chemical and electrochemical equilibrium	Crevice solution composition as a function of space and time
Sun et al.[17]	Experimental data by Alavi and Cottis	COMSOL Multiphysics	Dynamic pH distribution inside the crevice and corroded crevice shape
Engelhardt et al. [16]	Thermodynamic and kinetic data from elsewhere	Coupled environment approach	Concentration and potential distributions inside and outside crevice, critical permeability coefficient K_{cr}
Engelhardt and MacDonald [41]	Mathematical equations	Potential distribution inside a crevice obeys Ohm's law	w_{max} as a function of time and position from the anodic polarization curve
Walton et al. [4]	Experimental data by Alavi and Cottis, and Valdes-Mouldon	Mathematical reactive transport model	Potential, pH & anodic current density distribution
Stewart [23]	Own experiments + Valdes-Mouldon data	CF approach + CREVICER	Chemical concentration and potential fields of crevices
Kennell et al.[18]	Experimental data of Alavi and Cottis	IRDT+CCS theories	Predict the dynamic crevice pH profile
Anderko et al.[22]	Own tests for stainless steel 316L, AL6XN and alloy C-276	Repassivation theory	E_{rp} and E_{corr} from pitting corrosion rates

5 Summary

In this literature review crevice corrosion and its features are described, the main interest focused on approaching the modelling perspective of crevice corrosion. The review goes through some of the developed theories and modelling approaches performed during the last 40 years. All of the models use simplifications and assumptions to be able to answer the difficult dynamics of crevice corrosion. It seems that over time more and more modelling tools (FEM, COMSOL and other developed platforms) are being utilized, which is understandable considering the extensive work load needed in developing models from the start. The use of modelling tools is one solution for approaching the description of real systems. The flexibility and functionality of platforms needs to be checked, and the possibility of continuous updating is required. Statistical perspective of crevice corrosion reactions should be also considered in modelling.

The coupled environment theory, which takes into account the interaction between crevice and the external surfaces, has potential for predicting the crevice corrosion system. The modelling of crevice corrosion has yet great challenges to overcome, since the processes taking part in crevice corrosion are very dynamic with rapidly moving boundaries and rapidly changing chemistries and potentials. The more profound understanding of crevice corrosion processes is needed to tackle the difficulties involved.

References

- [1] Z. Szklarska-Smialowska, *Pitting and Crevice Corrosion*. NACE International, 2005.
- [2] L. L. Shreir, R. A. Jarman, and G. T. Burstein, *Corrosion (3rd Edition) Volumes 1-2*. Elsevier, 1994.
- [3] E. Mattsson, *Basic Corrosion Technology for Scientists and Engineers (2nd Edition)*. Maney Publishing for IOM3, the Institute of Materials, Minerals and Mining, 1996.
- [4] J. Walton, G. Cragolino, and S. Kalandros, "A numerical model of crevice corrosion for passive and active metals," *Corrosion Science*, vol. 38, no. 1, 1996.
- [5] D. R. Gunasegaram, M. S. Venkatraman, and I. S. Cole, "Towards multiscale modelling of localised corrosion," *International Materials Reviews*, vol. 59, no. 2, pp. 84–114, Jan. 2014.
- [6] S. Sharland, "A review of the theoretical modelling of crevice and pitting corrosion," *Corrosion Science*, vol. 27, no. 3, pp. 289–323, 1987.
- [7] G. Frankel and N. Sridhar, "Understanding localized corrosion," *Materials Today*, vol. 11, no. 10, pp. 38–44, 2008.
- [8] K. Heppner, "Prediction of the Crevice Corrosion Incubation Period of Passive Metals at Elevated Temperatures: Part I—Mathematical Model," *The Canadian Journal of Chemical Engineering*, vol. 80, no. October, pp. 849–856, 2002.
- [9] P. Jakobsen and E. Maahn, "Temperature and potential dependence of crevice corrosion of AISI 316 stainless steel," *Corrosion Science*, vol. 43, no. 9, pp. 1693–1709, Sep. 2001.
- [10] J. Soltis, "Passivity breakdown, pit initiation and propagation of pits in metallic materials – Review," *Corrosion Science*, vol. 90, pp. 5–22, Jan. 2015.
- [11] Y. Hisamatsu, "Pitting Corrosion of Stainless Steels in Chloride Solution," *USA-Japan Seminar*, p. 99, 1976.
- [12] J. R. Galvele, *Journal of the Electrochemical Society* 123, p. 123, 1976.
- [13] ASM International, *ASM Handbook Volume 13: Corrosion*. 1987.
- [14] A. Etor, "Electrochemical Measurement of Crevice Corrosion of Type AISI 304 Stainless Steel," Thesis, November, 2009.
- [15] National Association of Corrosion Engineers Research Committee, *Localized Corrosion*. 1971.
- [16] G. R. Engelhard, L. G. McMillion, and D. D. Macdonald, "A mathematical model for crevice corrosion under porous deposits," *Journal of Nuclear Materials*, vol. 379, no. 1–3, pp. 48–53, Sep. 2008.

- [17] W. Sun, L. Wang, T. Wu, and G. Liu, "An arbitrary Lagrangian–Eulerian model for modelling the time-dependent evolution of crevice corrosion," *Corrosion Science*, vol. 78, pp. 233–243, Jan. 2014.
- [18] G. F. Kennell, R. W. Evitts, and K. L. Heppner, "A critical crevice solution and IR drop crevice corrosion model," *Corrosion Science*, vol. 50, no. 6, pp. 1716–1725, Jun. 2008.
- [19] H. Pulkkinen, H. Apajalahti, S. Papula, J. Talonen, and H. Hänninen, "Pitting Corrosion Resistance of Mn-Alloyed Austenitic Stainless Steels," *Steel Research International*, vol. 85, no. 3, pp. 324–335, Mar. 2014.
- [20] A. Bouzoubaa, B. Diawara, V. Maurice, C. Minot, and P. Marcus, "Ab initio modelling of localized corrosion: Study of the role of surface steps in the interaction of chlorides with passivated nickel surfaces," *Corrosion Science*, vol. 51, no. 9, pp. 2174–2182, Sep. 2009.
- [21] L. DeJong, "Investigations of crevice corrosion scaling laws using microfabrication techniques and modeling," Thesis, August, 1999.
- [22] A. Anderko, N. Sridhar, L. T. Yang, S. L. Grise, B. J. Saldanha, and M. H. Dorsey, "Validation of localised corrosion model using real time corrosion monitoring in a chemical plant," *Corrosion Engineering, Science and Technology*, vol. 40, no. 1, pp. 33–42, Mar. 2005.
- [23] K. C. Stewart, "Intermediate Attack in Crevice Corrosion by Cathodic Focusing," Dissertation, August, 1999.
- [24] H.-K. Shu, F. M. Al-Faqeer, and H. W. Pickering, "Pitting on the crevice wall prior to crevice corrosion: Iron in sulfate/chromate solution," *Electrochimica Acta*, vol. 56, no. 4, pp. 1719–1728, Jan. 2011.
- [25] S. Lee, W. Kuang, and J. Mathews, "Monitoring Crevice Corrosion via the Coupling Current Part I: Detecting Crevice Activation, Inversion, and Inhibition," *Power Plant Chemistry*, vol. 15, no. 4, pp. 240–250, 2013.
- [26] L. Stockert and H. Boehni, *Materials Science Forum* 44/45, p. 313, 1989.
- [27] S. Sharland, C. Jackson, and A. Diver, "A finite-element model of the propagation of corrosion crevices and pits," *Corrosion Science*, vol. 29, no. 9, pp. 1149–1166, 1989.
- [28] N. J. Laycock, J. S. Noh, S. P. White, and D. P. Krouse, "Computer simulation of pitting potential measurements," *Corrosion Science*, vol. 47, no. 12, pp. 3140–3177, Dec. 2005.
- [29] S. Lee, "The coupled environment models for localized corrosions; Crevice corrosion and stress corrosion cracking," Dissertation of Pennsylvania State University, August, 2013.
- [30] J. Koryta, J. Dvorak, and L. Kavan, *Principles of Electrochemistry*. John Wiley and Sons Ltd., 1993.
- [31] K. Heppner, "Prediction of the Crevice Corrosion Incubation Period of Passive Metals at Elevated Temperatures: Part II—Model Verification and Simulation," *The Canadian Journal of Chemical Engineering*, vol. 80, no. October, pp. 857–864, 2002.

- [32] A.J. Betts, L.H. Boulton, "Crevice corrosion: review of mechanisms, modelling, and mitigation", The Institute of Materials, 1993.
- [33] C. G. Zoski, *Handbook of Electrochemistry*. Elsevier, 2007.
- [34] A. Alavi and R. Cottis, "The determination of pH, potential and chloride concentration in corroding crevices on 304 stainless steel and 7475 aluminium alloy," *Corrosion Science*, vol. 27, no. 5, pp. 443–451, 1987.
- [35] Valdes-Mouldon, Ph.D. Thesis, The Pennsylvania State University, 1987.
- [36] S. E. Lott and R. C. Alkire, "The Role of Inclusions on Initiation of Crevice Corrosion of Stainless Steel," *Journal of the Electrochemical Society*, vol. 136, no. 4, 1989.
- [37] N. Laycock, J. Stewart, and R. Newman, "The initiation of crevice corrosion in stainless steels," *Corrosion Science*, vol. 39, no. 1, pp. 1791–1809, 1997.
- [38] T. Hakkarainen, "A Model for Prediction of Possibility of Localised Corrosion Attack of Stainless Steels," *The NACE International Annual Conference and Exposition 1996*.
- [39] D. E. Williams, C. Westcott, and M. Fleischmann, "Stochastic Models of Pitting Corrosion of Stainless Steels," *Journal of the Electrochemical Society*, vol. 132, no. 8, pp. 1796–1804, 1985.
- [40] D. D. Macdonald, Lecture slides on the PDM on 7.-9.1.1015 at VTT in Espoo, Finland.
- [41] G. R. Engelhardt and D. D. Macdonald, "Possible distribution of potential and corrosion current density inside corroding crevices," *Electrochimica Acta*, vol. 65, pp. 266–274, Mar. 2012.
- [42] J. A. Beavers and N. G. Thompson, *Corrosion*. 43, 185, 1987.